

Non-linear dynamics of a pelagic ecosystem model with multiple predator and prey types

GEORGINA A. GIBSON^{1*}, DAVID L. MUSGRAVE² AND SARAH HINCKLEY³

¹SCHOOL OF FISHERIES AND OCEAN SCIENCE, UNIVERSITY OF ALASKA FAIRBANKS, FAIRBANKS, AK 99775-7220, USA, ²INSTITUTE OF MARINE SCIENCE, UNIVERSITY OF ALASKA FAIRBANKS, FAIRBANKS, AK 99775-7220, USA AND ³NOAA, NATIONAL MARINE FISHERIES SERVICE, ALASKA FISHERIES SCIENCE CENTER, 7600 SAND POINT WAY NORTHEAST, SEATTLE, WA 98115, USA

*CORRESPONDING AUTHOR: george@ims.uaf.edu

Received October 11, 2004; accepted in principle January 26, 2005; accepted for publication March 29, 2005; published online April 19, 2005

Using numerical techniques, we explored the dynamics of a one-dimensional, six-component nutrient–phytoplankton–zooplankton (NPZ) model in which zooplankton grazed on a mixed prey field. Five alternative functional forms were implemented to describe zooplankton grazing, and the form for predation on mesozooplankton was prescribed by a product of a specific predation rate (h) and the mesozooplankton concentration raised to a power (q), which we varied between one and two. With all five grazing functions, Hopf bifurcations, where the form of the solution transitioned between steady equilibrium and periodic limit cycles, persisted across the q – h parameter space. Regardless of the values of h and q , with some forms of the grazing function, we were unable to find steady equilibrium solutions that simultaneously comprised non-zero concentrations for all six model components. Extensions of Michaelis–Menten-based single resource grazing formulations to multiple resources resulted in periodic solutions for a large portion of the q – h space. Conversely, extensions of the sigmoidal grazing formulation to multiple resources resulted in steady solutions for a large portion of q – h parameter space. Our results demonstrate the consequences of the functional form of biological processes on the form of the model solutions. Both the steady or oscillatory nature of state variable concentrations and the likelihood of their elimination are important considerations for ecosystem-modelling studies, particularly when attempting to model an ecosystem in which multiple phytoplankton and zooplankton components are thought to persist simultaneously for at least a portion of the seasonal cycle.

INTRODUCTION

Since the historical works of Riley (Riley, 1946) and Steele (Steele, 1974), the use of nutrient–phytoplankton–zooplankton (NPZ) models as tools to understand temporal and spatial dynamics of marine ecosystems has become a common practice. Despite the many gross generalizations these models embody, they provide useful research tools to test the understanding of marine ecosystem functionality. Reflecting our increased understanding of the marine ecosystem, and in an effort to simulate observed dynamics left unexplained by simple three-component NPZ models, there has been a trend towards developing more sophisti-

cated ecosystem models with an increasing number of components and associated interactions. The ever-increasing availability of computational power has enabled the development of high resolution, three-dimensional, coupled biological–physical models that can perform realistic simulations of a marine ecosystem. Such coupled models are now frequently an integral part of research programs geared to understand ecosystem dynamics, e.g. the Global Ocean Ecosystem Dynamics experiment (GLOBEC) (Franks and Chen, 2001), the Joint Global Ocean Flux Study (Loukos *et al.*, 1997) and the North Pacific Marine Organization (Aita *et al.*, 2003).

Our conceptual view of the minimum complexity required to replicate observations constantly shifts, reflecting the continual refinement of our understanding of marine ecosystems. In the past, because of a more simplistic view of the marine ecosystem and following the Occams razor principle, marine ecosystem models were generally simple, zero- or one-dimensional, three-component NPZ models comprising nitrate, micro-phytoplankton and herbivorous mesozooplankton. Phytoplankton, however, are known to utilize both new (nitrate) and regenerated (ammonium) forms of inorganic nitrogen (Dugdale and Goering, 1967; Eppley and Peterson, 1979), and pico- and nanophytoplankton have been found to frequently contribute a large percentage of the total primary production (Johnson and Sieburth, 1979, 1982; Strom *et al.*, 2001). Because of the differing ability of the two phytoplankton groups to utilize the two nutrient sources, and to the different role each phytoplankton size fraction plays in the marine food web, both small and large phytoplankton are now frequently modelled independently in marine ecosystem models. The importance of microzooplankton, with their ability to feed on the small phytoplankton size fraction, has also been realized. This zooplankton size fraction is now thought to comprise the primary grazers (Dagg, 1993) controlling the chlorophyll standing stock in many regions (Landry and Hassett, 1982; Gifford and Dagg, 1988; Strom and Welschmeyer, 1991; Dagg, 1995).

Although the numerous variations of complex ecosystem models presented in the literature frequently share the same roots, they often differ substantially in the formulation of biological processes. Historically, the hyperbolic function first introduced by Monod (Monod, 1942) has been thought the most suitable for simulation of phytoplankton nutrient uptake (Wroblewski, 1977; Frost, 1987). Although more recently it has been shown that this is not the most appropriate functional form in a multiple nutrient situation (Flynn, 2003), it is still the most commonly used in marine ecosystem models (Hurtt and Armstrong, 1999; Lancelot *et al.*, 2000; Kishi *et al.*, 2001). There is a similar, and older discourse regarding which functional forms are most appropriate for simulating grazing, defined here as zooplankton grazing on phytoplankton, and smaller zooplankton, or 'predation', defined as mesozooplankton mortality owing to consumption by undefined higher trophic levels. Predation is often simulated by using either a linear formulation that represents a predator whose biomass does not fluctuate (Evans and Parslow, 1985; Fasham *et al.*, 1990) or a quadratic formulation that represents a predator whose biomass is proportional to that of the zooplankton (Fasham, 1995; Edwards, 2001). Hyperbolic (Frost, 1987; Fasham *et al.*, 1993) and sigmoidal formulations (Malchow, 1994) have also been used to

simulate predation, although not as commonly, perhaps because of the additional parameters and associated assumptions these formulations would require. Historically, the formulation for zooplankton grazing has also taken several different forms. The hyperbolic formulation (Ivlev, 1961; Frost, 1987) was a common choice. However, in an effort to prevent complete prey elimination owing to zooplankton grazing, formulations were developed to provide rare prey with a refuge from grazing pressure. The most notable of the prey refuge functions are the 'threshold' function (Steele, 1974; Mullin and Fuglister, 1975; Wroblewski, 1977), which incorporates a critical prey concentration below which grazing ceases, and the sigmoidal function, in which the grazing rate is reduced at low prey concentrations (Evans and Parslow, 1985; Steele and Henderson, 1992; Denman and Peña, 1999). There is evidence that at least some species of zooplankton do exhibit behaviour consistent with this line of thought (Frost, 1972, 1975; Strom, 1991; Gismervik and Andersen, 1997). Such observations are, however, usually made on individual species that are fed known prey types, and do not necessarily reflect the behaviour of the zooplankton community at large. Nevertheless, the addition of a grazing refuge to a grazing function is popular with the modelling community because it often overcomes the problem of prey elimination. With the advent of multiple prey marine ecosystem models, it is becoming increasingly common to see extensions of the single resource grazing functions in order to simulate zooplankton grazing on a mixed prey field (Ambler, 1986; Fasham *et al.*, 1990; Ryabchenko *et al.*, 1997; Chifflet *et al.*, 2001; Denman and Peña, 2002). A comprehensive review of the grazing functional response for zooplankton grazing on single and multiple nutritional resources (prey items) is provided by Gentleman *et al.* (Gentleman *et al.*, 2003).

Despite a rapid trend towards more realistic marine ecosystem models, in which zooplankton are presented with multiple nutritional resources, investigations into the fundamental dynamics of these newer models have been limited (Armstrong, 1994; Ryabchenko *et al.*, 1997; Yool, 1998). Over the past few decades, the application of non-linear systems dynamics has provided a basis for understanding the behaviour of ecosystem models (May, 1973; Oaten and Murdoch, 1975; Edwards and Brindley, 1996; Edwards *et al.*, 2000). The formulations for both zooplankton grazing (Franks *et al.*, 1986) and predation on zooplankton (Steele and Henderson, 1992; Edwards and Yool, 2000) have been found to influence the fundamental dynamics of simple NPZ model, determining whether a model's time-dependent behaviour will approach steady state or exhibit oscillatory behaviour, such as periodic limit cycles. Furthermore, incorporating moderate levels of vertical diffusion

into a purely biological NPZ model has been shown to impart model stability (Edwards *et al.*, 2000), an important consideration for the realm of coupled biophysical models. Without a good understanding of the fundamental behaviour of the more complex ecosystem models now commonly employed in ecosystem studies, time-dependent behaviour simulated with coupled biological-physical models, as in periodic or chaotic solutions, could be interpreted as due to variable physical forcing rather than as an inherent property of an ecosystem model. It is important that we extend our understanding of NPZ system dynamics to these more complex models and develop an appreciation of how choices of formulations for simulating biological processes can affect their behaviour.

Here, we explore the fundamental non-linear dynamics of an intermediately complex marine ecosystem model in which zooplankton grazers can feed on multiple prey types. Time-series solutions are examined, and their behaviour classified with respect to their non-linear dynamics and structural stability as steady, limit cycle (periodic) or chaotic. Our analysis is based on a six-component model, subjected to stationary physical forcing (vertical light and mixing profiles). One of our long-term interests is to include our biological model into a simulation with realistic three-dimensional physics in the coastal Gulf of Alaska. Therefore, where possible, we have used biological and physical parameter values that are realistic for that region. We compare model behaviour with alternative functional forms for zooplankton grazing over a realistic range of specific predation rates [$h = 0-2.4 \text{ (g C m}^{-3}\text{)}^{1-q} \text{ day}^{-1}$] and predation exponents ($1 \leq q \leq 2$).

METHOD

Model structure

To investigate the influence on model dynamics of alternative grazing and mortality functions when zooplankton are able to graze on a mixed prey field, we developed a six-component model (Fig. 1) that simulated the exchange of nitrogen ($\mu\text{M N}$) between two classes of phytoplankton, small ($<8 \mu\text{M}$, P_1) and large ($>8 \mu\text{M}$, P_2); two classes of zooplankton, microzooplankton (Z_1) and mesozooplankton (Z_2); and two types of dissolved inorganic nitrogen, nitrate (N_1) and ammonium (N_2). Both size classes of zooplankton were allowed to graze on multiple prey types. This model was developed from the three-component NPZ model whose stability has previously been investigated (Edwards *et al.*, 2000). We selected this model because of the simplicity of its functional forms. We increased model complexity by adding a second phytoplankton and zooplankton component and splitting the nutrient compo-

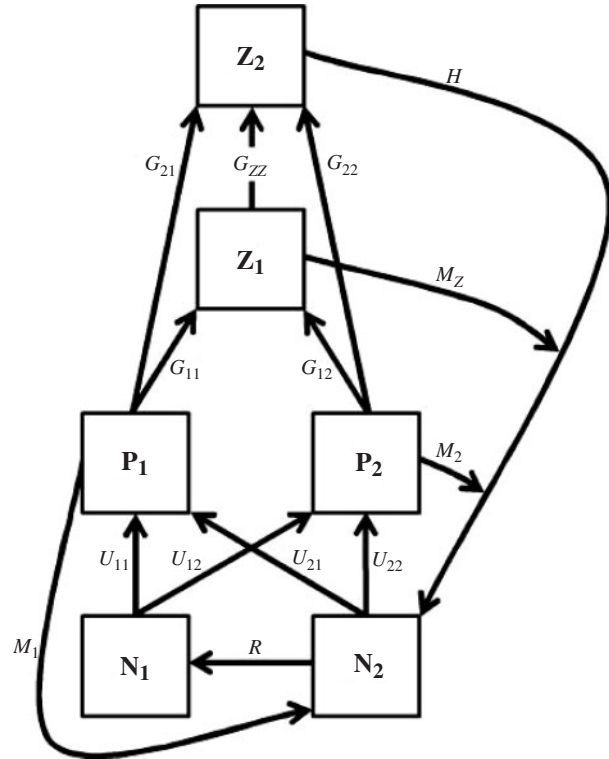


Fig. 1. Interactions within the six-component model; nitrate (N_1), ammonium (N_2), small phytoplankton (P_1), large phytoplankton (P_2), microzooplankton (Z_1) and mesozooplankton (Z_2). Arrows indicate the direction of material flow. Biological processes, i.e. grazing (G), nutrient uptake (U), mortality (M), predation (H) and nutrient regeneration (R) associated with each arrow are indicated. See Table II for explanation of suffixes. Note that for simplicity, zooplankton assimilation efficiencies have been omitted.

nent into nitrate and ammonium. The one-dimensional model was spatially explicit in the vertical, with a resolution of one meter and an extent of one hundred meters ($z_i = 1 \text{ m}$, 2 m , 3 m , \dots 100 m). The model was a closed system with no net inputs or outputs. Therefore, the total nitrogen content, summed over all depths, was constant at all times ($N_T = P_1 + P_2 + Z_1 + Z_2 + N_1 + N_2$). We feel that this is not an unrealistic assumption to make considering the vertical extent of the model. Each model component was mixed down its concentration gradient, the extent of mixing being determined by the vertical diffusion profile described below. With every simulation, the concentration of nitrate (N_1) at depth did not diverge significantly from its initial concentration. This meant that it was unnecessary to assume a nutrient source to resupply the mixed layer, an approach commonly taken in homogeneous mixed-layer models (Fasham *et al.*, 1990; Steele and Henderson, 1992) which solve the biological equations only for one-depth level. Potential losses from the system (i.e. mortality, predation and egestion) were treated as inputs to the ammonium pool; no detrital pool was explicitly modelled. Initial concentrations for all model components were taken to be

vertically homogeneous at 2 µg chlorophyll *a* L⁻¹ for both phytoplankton groups, 15 µg C L⁻¹ for both zooplankton groups, 10 µM N for nitrate and 1 µM N for ammonium. Based on observational results from the GLOBEC coastal Gulf of Alaska program (Strom *et al.*, 2001; Weingartner *et al.*, 2002), these values were considered reasonable representations of conditions in the coastal Gulf of Alaska during spring (May). To enable material flow between the phytoplankton, zooplankton and nutrient components, we used a common currency of nitrogen and assumed a C : N ratio of 106:16 (Redfield *et al.*, 1963) and a C : chlorophyll *a* ratio of 55:1 (Frost, 1987). This gave initial phytoplankton and zooplankton concentrations of 1.386 and 0.189 mmol N m⁻³, respectively.

Formulation

The purely biological dynamics are shown below in equations (1)–(6). As discussed later, these biological dynamics are also subjected to vertical mixing within the model [equation (7)].

Nutrient equations

Nitrate (n_1) and ammonium (n_2) dynamics were described by

$$\frac{dn_1}{dt} = -U_{11} - U_{12} + R \quad (1)$$

$$\begin{aligned} \frac{dn_2}{dt} = & -U_{11} - U_{22} + M_1 + M_2 + M_Z + H \\ & + (1 - \gamma_1) \cdot (G_{11} + G_{12}) + (1 - \gamma_2) \\ & \cdot (G_{21} + G_{22} + G_{zz}) - R \end{aligned} \quad (2)$$

where γ_1 and γ_2 represent zooplankton grazing efficiency for microzooplankton and mesozooplankton, respectively. In these and the following equations, U , M , G , H and R represent transformation rates of nitrogen owing to nutrient uptake, mortality, grazing, predation and the regeneration of ammonium to nitrate, respectively. Details of the formulations for the transformation rates and definitions of the subscripts are presented in Table I, and parameter values associated with the formulations are given in Table II. Uptake of both nitrate and of ammonium was modelled by using a Monod (Monod, 1942) formulation, the classic saturation response with increased concentration of resource. The inhibition of nitrate uptake owing to the presence of ammonium was simulated by using the exponential function introduced by Wroblewski (Wroblewski, 1977). Following similar studies of this nature (Edwards and Brindley, 1999; Edwards *et al.*, 2000), no detrital component was explicitly modelled. Edwards (Edwards, 2001)

found that if zooplankton were unable to graze on detritus, as is often the case in marine ecosystem models (Leonard *et al.*, 1999; Chifflet *et al.*, 2001; Kishi *et al.*, 2001), the inclusion of this component made little difference to the observed model dynamics. With this simplified view of the regeneration loop, we assume that losses from the phytoplankton and zooplankton model components are instantaneously remineralized back to ammonium, and that the regeneration of ammonium to nitrate occurs at a specific constant rate (r). Parameter values (Table II), most representative of the coastal Gulf of Alaska ecosystem were selected. However, knowledge of parameter values in this region is limited. Where possible, observational values were used, but in their absence, values were selected that fell within the range presented in the marine ecosystem modelling literature.

Phytoplankton equations

Phytoplankton dynamics were described by

$$\frac{dP_1}{dt} = U_{11} + U_{21} - M_1 - G_{11} - G_{21} \quad (3)$$

$$\frac{dP_2}{dt} = U_{12} + U_{22} - M_2 - G_{12} - G_{22} \quad (4)$$

The phytoplankton size division ($P_1 < 8\mu\text{M} < P_2$) was chosen to mimic that selected by Strom *et al.* (Strom *et al.*, 2001), who have conducted the majority of the limited work on phytoplankton and microzooplankton processes in the coastal Gulf of Alaska. Reflecting observations in this ecosystem (Strom *et al.*, 2001), no significant difference between the maximum growth rate of the two phytoplankton size groups was assumed. A P_{max} of 2 day⁻¹ was assigned to both size classes, which seems appropriate given the ranges (0.54–2.21 day⁻¹) found for the total chlorophyll size fraction in this region during spring (Strom *et al.*, 2001). Daily average phytoplankton growth was assumed to be simultaneously limited by the availability of nutrients and photosynthetically active radiation (PAR). The attenuation of PAR below the sea surface was simulated by using the exponential decay function ($e^{-z \cdot k_{\text{ext}}}$) after Edwards *et al.* (Edwards *et al.*, 2000), where z is depth and is positive downwards. A light extinction coefficient ($k_{\text{ext}} = 0.07 \text{ m}^{-1}$) was chosen which gave an e-folding depth ($1/k_{\text{ext}}$) of 14.3 m and puts the midpoint of the euphotic zone ($2.3/k_{\text{ext}}$) at 33 m (Fig. 2). As discussed above, the dependence of phytoplankton growth on nitrate and ammonium availability were simulated with the saturating Monod function and the ammonium inhibition function (Wroblewski, 1977). Following Wroblewski (Wroblewski, 1977), and most ecosystem models since, we assigned the inhibition parameter (ψ) a value of 1.462

Table I: Biological processes used in the six-component model

Process	Symbol	Formulation		
P_X uptake of N_1	U_{1X}	$P_X \cdot P_{\max X} \cdot e^{-z \cdot k_{cst}} \cdot \frac{N_1 \cdot e^{-\psi N_2}}{k_{1X} + N_1}$		
P_X uptake of N_2	U_{2X}	$P_X \cdot P_{\max X} \cdot e^{-z \cdot k_{cst}} \cdot \frac{N_2}{k_{2X} + N_2}$		
Natural mortality of P_X	M_X	$m_X \cdot P_X$		
Natural mortality of Z_1	M_Z	$m_Z \cdot Z_1$		
Higher predation on Z_2	H	$h \cdot Z_2^q$		
N_2 regeneration, N_1	R	$r \cdot N_2$		
Zooplankton grazing	G	See below		

Grazing function	Capture efficiency	Z_1 grazing on P_X (G_{YX})	Z_2 grazing on Z_1 (G_{ZZ})	Literature example
I	Constant	$i_{\max} Z_Y \cdot \frac{\sum_{X=1,2} c_{1X} P_X}{k_{31} + \sum_{X=1,2} c_{1X} P_X} \cdot \frac{c_{1X} P_X}{\sum_{X=1,2} c_{1X} P_X}$	$i_{\max} Z_2 \cdot \frac{\sum_{X=1,2} c_{2X} P_X + c_{ZZ} Z_1}{k_{32} + \sum_{X=1,2} c_{2X} P_X + c_{ZZ} Z_1} \cdot \frac{c_{ZZ} Z_1}{\sum_{X=1,2} c_{2X} P_X + c_{ZZ} Z_1}$	Murdoch (1973)
II	Constant	$i_{\max} Z_Y \cdot \frac{\sum_{X=1,2} c_{1X} P_X - \theta}{k_{31} + \sum_{X=1,2} c_{1X} P_X - \theta} \cdot \frac{c_{1X} P_X}{\sum_{X=1,2} c_{1X} P_X}$	$i_{\max} Z_2 \cdot \frac{\sum_{X=1,2} c_{2X} P_X + c_{ZZ} Z_1 - \theta}{k_{32} + \sum_{X=1,2} c_{2X} P_X + c_{ZZ} Z_1 - \theta} \cdot \frac{c_{ZZ} Z_1}{\sum_{X=1,2} c_{2X} P_X + c_{ZZ} Z_1}$	Frost (1987) Lancelot <i>et al.</i> (2000)
III	Variable	$i_{\max} Z_Y \cdot \frac{\sum_{X=1,2} \varepsilon_{1X} P_X}{k_{31} + \sum_{X=1,2} \varepsilon_{1X} P_X} \cdot \frac{\varepsilon_{1X} P_X}{\sum_{X=1,2} \varepsilon_{1X} P_X}$	$i_{\max} Z_2 \cdot \frac{\sum_{X=1,2} \varepsilon_{2X} P_X + \varepsilon_{ZZ} Z_1}{k_{32} + \sum_{X=1,2} \varepsilon_{2X} P_X + \varepsilon_{ZZ} Z_1} \cdot \frac{\varepsilon_{ZZ} Z_1}{\sum_{X=1,2} \varepsilon_{2X} P_X + \varepsilon_{ZZ} Z_1}$	Chifflet <i>et al.</i> (2001) Fasham <i>et al.</i> (1990)
IV	Constant	$i_{\max} Z_Y \cdot \frac{\left(\sum_{X=1,2} c_{1X} P_X \right)^2}{k_{31}^2 + \left(\sum_{X=1,2} c_{1X} P_X \right)^2} \cdot \frac{c_{1X} P_X}{\sum_{X=1,2} c_{1X} P_X}$	$i_{\max} Z_2 \cdot \frac{\left(\sum_{X=1,2} c_{2X} P_X + c_{ZZ} Z_1 \right)^2}{k_{32}^2 + \left(\sum_{X=1,2} c_{2X} P_X + c_{ZZ} Z_1 \right)^2} \cdot \frac{c_{ZZ} Z_1}{\sum_{X=1,2} c_{2X} P_X + c_{ZZ} Z_1}$	Strom and Loukos (1998) Denman and Peña (2002)
V	Constant	$i_{\max} Z_Y \cdot \frac{\left(\sum_{X=1,2} c_{1X} P_X^2 \right)^2}{k_{31}^2 + \left(\sum_{X=1,2} c_{1X} P_X^2 \right)^2} \cdot \frac{c_{1X} P_X^2}{\sum_{X=1,2} c_{1X} P_X^2}$	$i_{\max} Z_2 \cdot \frac{\sum_{X=1,2} c_{2X} P_X^2 + c_{ZZ} Z_1^2}{k_{32}^2 + \sum_{X=1,2} c_{2X} P_X^2 + c_{ZZ} Z_1^2} \cdot \frac{c_{ZZ} Z_1^2}{\sum_{X=1,2} c_{2X} P_X^2 + c_{ZZ} Z_1^2}$	Ryabchenko <i>et al.</i> (1997)

Parameter definitions and values are given in Table II. X and Y can be 1 or 2 to represent the two classes of phytoplankton and zooplankton, respectively.

($\mu\text{M N}$)⁻¹. Reflected in their half-saturation constants, the two phytoplankton size fractions were assumed to have different preferences for the two nitrogen pools. Small phytoplankton, generally more proficient at utilizing low levels of nutrients (Evans and Parslow, 1985), had a smaller half-saturation uptake for ammonium than large phytoplankton. Small phytoplankton's half-saturation uptake for nitrate was considered larger than for ammonium, reflecting a general preference for ammonium (Legendre and Rassoulzadegan, 1995). Large phytoplankton had a smaller half-saturation uptake for nitrate than ammonium because in cold water this size class has been found to preferentially take up nitrate even when ammonium is present (Lomas and Glibert, 1999), although more recent studies indicate otherwise (Flynn, 1999; Flynn, 2003).

Both phytoplankton size fractions suffered losses because of natural mortality and zooplankton grazing. Mortality of each phytoplankton size class was taken to be a constant fraction of the standing stock and was assumed to be higher for the smaller cells. Both size fractions could potentially be grazed by either of the zooplankton size fractions. The form of the grazing function varied and is discussed further below.

Zooplankton equations

The dynamics of the two zooplankton components were described by

$$\frac{dZ_1}{dt} = \gamma_1 \cdot (G_{11} + G_{12}) - G_{ZZ} - M_Z \quad (5)$$

Table II: Parameter values used in the model

Parameter	Symbol	Values		Units									
		X = 1	X = 2										
Maximum growth rate of P _X	P _{maxX}	2	2	day ⁻¹									
P _X half-saturation constant for N ₁	k _{1X}	.75	.5	μM N									
P _X half-saturation constant for N ₂	k _{2X}	.5	1	μM N									
Inhibition parameter for U ₁ by N ₂	ψ	1.462		(μM N) ⁻¹									
Remineralization rate	r	0.05		day ⁻¹									
Light extinction coefficient	k _{ext}	0.07		m ⁻¹									
Mmoles N m ⁻³ : mg C m ⁻³	n	0.0126		—									
		Y = 1	Y = 2										
Maximum ingestion rate	i _{maxY}	1.2	.7	day ⁻¹									
Assimilation efficiency of Z _Y	γ _Y	0.4	0.3	—									
Z _Y half-saturation grazing coefficient	k _{3Y}	30·n	60·n	mmoles N m ⁻³									
Z _Y capture efficiency for P _X	e _{YX}	<table border="1"> <tr> <td></td> <td>Y=1</td> <td>Y=2</td> </tr> <tr> <td>X=1</td> <td>1</td> <td>.2</td> </tr> <tr> <td>X=2</td> <td>.7</td> <td>.7</td> </tr> </table>			Y=1	Y=2	X=1	1	.2	X=2	.7	.7	—
	Y=1	Y=2											
X=1	1	.2											
X=2	.7	.7											
Z ₂ capture efficiency for Z ₁	e _{ZZ}	1											
		Y = 1	Y = 2										
Variable Z _Y capture efficiency for P _X	ε _{YX}	$\frac{e_{YX} \cdot P_X}{\sum_{X=1,2} e_{YX} P_X}$		$\frac{e_{YX} \cdot P_X}{e_{ZZ} \cdot Z_1 + \sum_{X=1,2} e_{YX} P_X}$									
Variable Z ₂ capture efficiency for Z ₁	ε _{ZZ}	$\frac{e_{ZZ} \cdot Z_1}{e_{ZZ} \cdot Z_1 + \sum_{X=1,2} e_{YX} P_X}$											
Feeding threshold concentration	θ	0.05·n		mmoles N m ⁻³									
		X = 1	X = 2										
Natural mortality rate of P _X	m _X	0.2	0.1	day ⁻¹									
Natural mortality rate of Z ₁	m _z	0.08		day ⁻¹									
Specific predation rate	h	0-2.4 = 0.04 ^(q-1) - 0.1908 ^(q-1)		(g C m ⁻³) ^{1-q} day ⁻¹ (mmoles N m ³) ^{1-q} day ⁻¹									
Predation exponent	q	1-2		—									

X and Y can be 1 or 2 to represent the two classes of phytoplankton and zooplankton, respectively.

$$\frac{dZ_2}{dt} = \gamma_2 \cdot (G_{21} + G_{22} + G_{ZZ}) - H \quad (6)$$

The mesozooplankton fraction (Z₂) was considered to represent mainly coastal copepods common in the coastal Gulf of Alaska, while the microzooplankton frac-

tion (Z₁) was considered to consist of mainly heterotrophic dinoflagellates and ciliates. The diet of copepods is known to be very diverse (Kleppel, 1993), and members of this group can potentially feed on microzooplankton (Gifford and Dagg, 1988; Jonsson and Tiselius, 1990), large phytoplankton such as diatoms

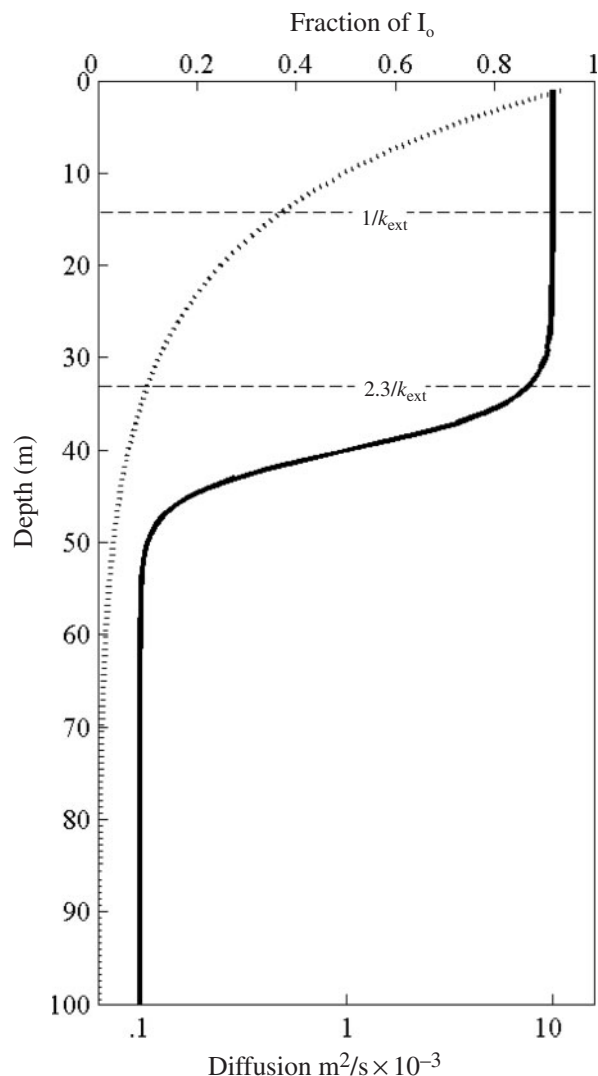


Fig. 2. Vertical diffusion and light extinction profiles used in the model. The solid line represents the diffusion profile and the dotted line represents the light profile. The important depths associated with these stationary forcing functions are the e-folding depth ($1/k_{\text{ext}}$) for the light extinction, the midpoint of the euphotic zone ($2.3/k_{\text{ext}}$), the top of the pycnocline at ~ 30 m and the bottom of the pycnocline at ~ 50 m.

(Corkett and McLaren, 1978; Dagg and Walser, 1987; Dagg, 1995) and even nanoplankton (Kleppel, 1993; Kleppel *et al.*, 1996). Microzooplankton are also able to consume a wide range of particle sizes. Observational studies in the coastal Gulf of Alaska (Strom *et al.*, 2001) have found that microzooplankton were just as effective at feeding large plankton ($>8 \mu\text{m}$) as they were at feeding on small plankton ($<8 \mu\text{m}$). To reflect our understanding of this ecosystem, mesozooplankton were assumed capable of grazing on both small and large phytoplankton and microzooplankton. Microzooplankton were

assumed able to graze on both phytoplankton size fractions. Capture efficiency parameters were chosen to represent an ecosystem in which, because of size restrictions, microzooplankton could capture small phytoplankton with a greater efficiency than large phytoplankton, and mesozooplankton could capture microzooplankton, large phytoplankton and small phytoplankton with a decreasing order of efficiency. Microzooplankton were assigned a maximum grazing rate of 1.2 day^{-1} , which was the maximum found for this size class in the coastal Gulf of Alaska in May (Strom *et al.*, 2001). Considering that mesozooplankton grazing can be substantially less than microzooplankton grazing (Dagg, 1995), and following the precedent set in previous ecosystem modelling studies (Frost and Franzen, 1992; Leonard *et al.*, 1999; Kishi *et al.*, 2001), the maximum grazing rate assigned to the mesozooplankton was less than for the microzooplankton (0.7 day^{-1}). The microzooplankton were also able to respond more rapidly (smaller half-saturation constant) to increases in phytoplankton biomass than the mesozooplankton, whose growth was assumed to be not as tightly coupled to the phytoplankton.

In the original three-component model, on which our model was based (Franks *et al.*, 1986), grazing by the single zooplankton on the single phytoplankton group is assumed to follow an Ivlev functional form similar to the hyperbolic formulation produced with a Michaelis–Menten function. Here, five alternative functional forms for zooplankton grazing on multiple prey types were implemented, all of which had previously been used in ecosystem modelling studies. The formulations for each grazing function are presented in Table II. Schematics to illustrate the essential differences between each of these functions are presented in Fig. 3. Grazing functions I, II and III are extensions of the ‘Michaelis–Menten’ and ‘Threshold’ single resource functional responses curves to multiple nutritional resources (prey items). Functions IV and V are two alternative extensions of the single resource sigmoidal function to multiple prey types. Function I never provides rare prey with a reprise from grazing. Functions II and IV provide prey with a reprise from zooplankton grazing pressure, only if the combined concentration of all prey resources is sufficiently small. Functions III and V permit scarce prey with a reprise from grazing pressure even if concentrations of alternative prey items are high. With function V, this prey refuge persists even when only one prey type remains. With function III, once the prey field has been decreased to a single nutritional resource, the functional form for grazing is similar to function I.

Grazing functions I and II used in this research have been categorized as ‘Class 1 multiple functional responses’ by Gentleman *et al.* (Gentleman *et al.*, 2003) because they

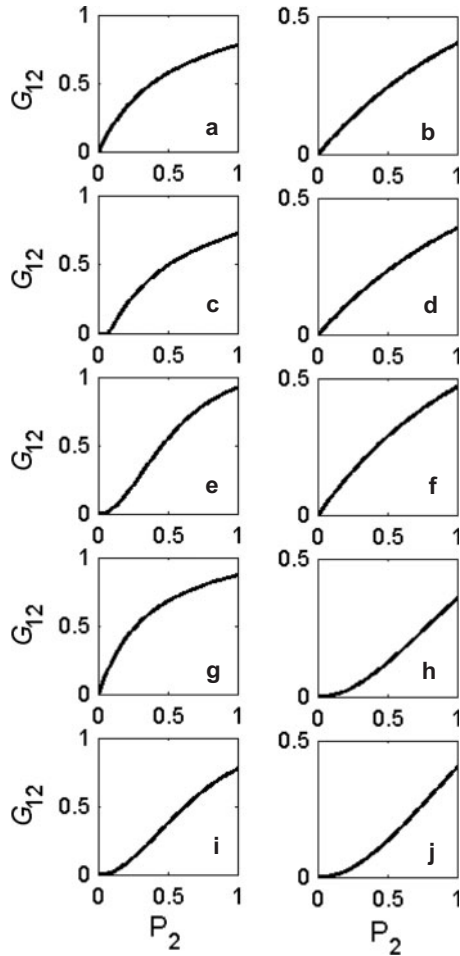


Fig. 3. Schematic of the key differences between the five grazing functions implemented in the model. Grazing by Z_1 on P_2 when $P_1 = 0$ (left column) and when $P_1 = 1$ (right column) with grazing function I (a and b), function II (c and d), function III (e and f), function IV (g and h) and function V (i and j).

assume passive selection and no switching. Grazing function III is also an extension of the ‘Michaelis–Menten’ curve. However, this function incorporates ‘capture efficiencies’ (or preferences) that vary with prey ratios. This function is categorized as a ‘Class 3 (proportion based) multiple functional response’ (Gentleman *et al.*, 2003) because the capture efficiencies are density dependent, varying with the densities of other resources. Function V is a ‘Class 2 (Sigmoidal I) multiple functional response’ (Gentleman *et al.*, 2003). Grazing function IV has not been classified under this scheme, however, its nutritional intake behaviour is similar to grazing function II.

In addition to grazing pressure by mesozooplankton, microzooplankton experienced natural mortality at a constant specific rate. In reality, mesozooplankton also suffer losses owing to natural mortality and predation by

higher trophic levels. However, because of the uncertainty associated with both of these terms, we combined them into a single term ($H = h \cdot Z_2^q$), which is referred to throughout as ‘predation’. H is effectively the model closure term. Common choices for the predation exponent are $q = 1$ (Evans and Parslow, 1985; Fasham *et al.*, 1990) or $q = 2$ (Denman and Gargett, 1995; Fasham, 1995). The former parameterization represents a predator that exhibits a constant response to zooplankton prey numbers (linear closure), this could be thought of as a simple filter-feeding strategy. The later parameterization (quadratic closure) is thought to represent a predator that exhibits an ambush-feeding strategy, being attracted to large concentration of zooplankton and less inclined to feed at low concentrations. It is thought, however (Edwards and Bees, 2001), that because a predators’ effective reaction distance varies with the turbulent energy dissipation rate, the proportion of predators adopting each strategy will vary in a continuous fashion depending on the environmental and physical conditions. Non-steady model solutions are not necessarily eliminated with the use of quadratic closure, as was once thought (Steele and Henderson, 1992). Rather, much of a model’s dynamical behaviour is generic, occurring for any exponent of closure between one and two (Edwards and Bees, 2001). In light of this finding, we chose to explore the dynamics of our model with a non-integer predation exponent that was varied from linear to quadratic ($1 \leq q \leq 2$), while the specific predation rate (h) was varied over a biologically realistic range [$0.05\text{--}2.4 \text{ (g C m}^{-3}\text{)}^{1-q} \text{ day}^{-1} = 0.04^{(q-1)} - 0.1908^{(q-1)} \text{ mmoles N m}^{-3}\text{)}^{1-q} \text{ day}^{-1}$].

Diffusion

Within the model, the purely biological dynamics [equations (1)–(6)] were subjected to vertical mixing. This physical forcing was represented by the addition of a term [equation (7)] to each of the six biological equations.

$$\frac{\partial}{\partial z} \left(K \frac{\partial C}{\partial z} \right) \quad (7)$$

where z is depth, K is the vertical diffusion coefficient and C represents each of the model components P_1 , P_2 , Z_1 , Z_2 , N_1 and N_2 .

It is known that the magnitude of diffusion can modify the non-linear dynamics of an NPZ model (Edwards *et al.*, 2000). Therefore, to best understand the NPZ model dynamics without the complications of temporally varying physical forcing, model behaviour was explored in the presence of temporally constant but spatially varying

levels of diffusion. Diffusion acted at each of the models at 100 depth levels to mix each of the model components down their concentration gradient. The diffusion at each depth was determined with the following equation:

$$K\hat{v}(z) = K\hat{v}_b - \left(\frac{K\hat{v}_b - K\hat{v}_m}{\tanh(\Phi_{100}) - \tanh(\Phi_1)} \right) - \left(\frac{K\hat{v}_b - K\hat{v}_m}{\tanh(\Phi_{100}) - \tanh(\Phi_1)} \right) \cdot \tanh\left(\frac{-\Phi(z)}{\psi} \right) \tag{8}$$

Although simplified, this approach provided a somewhat realistic structure, with a smooth transition between the higher coefficient of diffusion ($K\hat{v}_m = 1 \times 10^{-3} \text{ m}^2 \text{ s}^{-1}$) in the surface mixed layer and the smaller background value ($K\hat{v}_b = 1 \times 10^{-5} \text{ m}^2 \text{ s}^{-1}$) below (Fig. 2). The shape parameters, $\Phi(z) = z - 40$ (where $z = 1, 2, 3, \dots, 100$) and $\psi = 5$, which respectively define the position and thickness of the pycnocline, were used to give a mixed layer of about 40 m and a pycnocline about 20 m thick, appropriate conditions for the coastal Gulf of Alaska in spring (Luick *et al.*, 1987). No flux boundary conditions were enforced at the upper and lower boundaries, i.e.

$$\begin{aligned} \text{At } z = 0 \text{ and } 100 \text{ m, } K\hat{v} \frac{\partial P_1}{\partial z} &= K\hat{v} \frac{\partial P_2}{\partial z} = K\hat{v} \frac{\partial Z_1}{\partial z} = K\hat{v} \frac{\partial Z_2}{\partial z} \\ &= K\hat{v} \frac{\partial N_1}{\partial z} = K\hat{v} \frac{\partial N_2}{\partial z} = 0 \end{aligned}$$

It is important to note that for simplicity, the ability of mesozooplankton to swim or maintain a position in the water column through buoyancy control is not considered at this time.

Analysis

The dynamics of our model were compared when five alternative functional forms for zooplankton grazing (G) were implemented, and the predation exponent (q) and the specific predation rate (h) in the predation term (H) were systematically varied over a range of 1–2 and 0.05–2.4 ($\text{g C m}^{-3} \text{ day}^{-1} = 0.04^{(q-1)} - 0.1908^{(q-1)}$) ($\text{mmoles N m}^{-3} \text{ day}^{-1}$, respectively, following a previous study into model dynamics (Edwards and Bees, 2001). For each model simulation, we attempted to find the steady solutions of the discretized non-linear system of six equations iteratively. Each model was initially run for 300 time steps (days), and the resulting solution provided as a starting guess to a numerical solver of the steady state solution [equations (1)–(6) with the left hand sides set to zero]. Following Edwards *et al.* (Edwards *et al.*, 2000), for a model to be classified as steady, the associated time-

derivative terms were required to be $<10^{-4}$. Models that failed to converge to a steady solution were run for a further 700 days, and the time series solution on the 1000th day was provided to the numerical solver. These solutions were then reclassified. Any solution which could not be classified as steady was manually examined, at the 25 m depth, to determine if behaviour was periodic (limit cycles) or something more complex. This process of time-stepping solutions for 1000 days followed by the examination of the solution trajectory was repeated until we were confident that the solutions were indeed limit cycles and not anything more complex. The last 500 days of all non-steady solutions were used to determine the period of oscillations.

RESULTS

Model behaviour was dependent on the total predation experienced by the mesozooplankton ($H = h \cdot Z_2^q$), rather than just on the predation exponent (q) or the specific predation rate (h) (Fig. 4). The relationship between the predation rate and the two predation parameters was dependent on the concentration of Z_2 . As the concentration of Z_2 increased, H became more dependent on h than q . Relatively high predation on mesozooplankton resulted when the predation exponent (q) was close to one (linear predation) or when the specific predation rate (h) was large. Conversely, relatively low predation resulted when the predation exponent approached two (quadratic predation) or the specific predation rate was small.

With some of the grazing functions (I, II and IV), it was not common to have all six model components existing simultaneously; solutions often comprised negligible concentrations (scaled concentrations $<10^{-6}$) of at least one model component (Fig. 5). The structural composition of

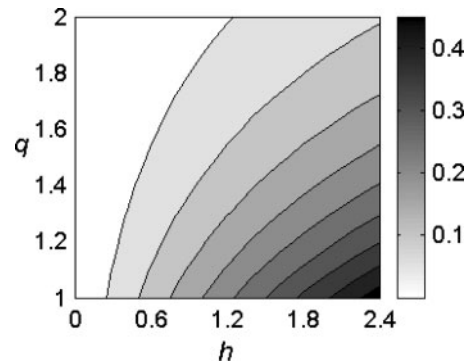


Fig. 4. Visual qualification of predation on mesozooplankton ($H = h \cdot Z_2^q$) over h and q parameter space. Non-dimensional mesozooplankton concentration (Z_2) was set to 0.1. Note that as the concentration of Z_2 is increased, H will become more dependent on h than q .

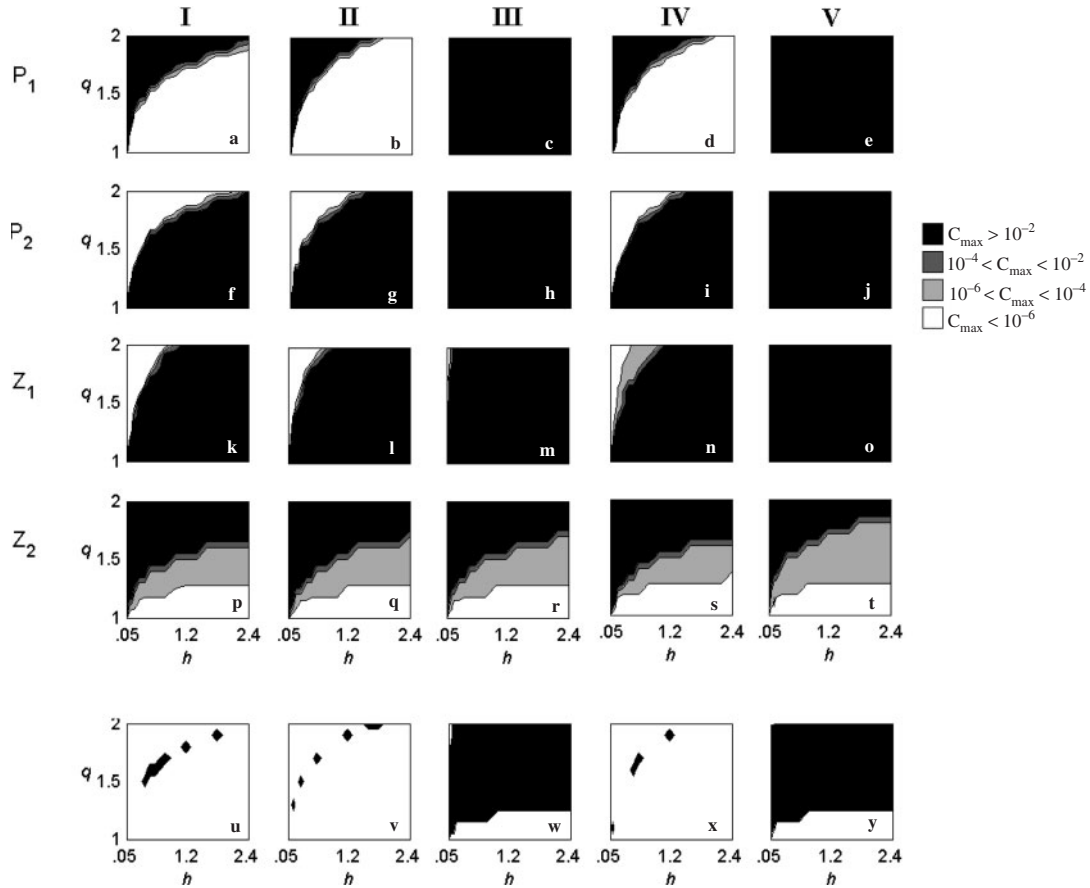


Fig. 5. Maximum concentration of the four plankton components (mmoles N m^{-3}). If solutions were steady, the maximum plankton concentrations over all depths at equilibrium were used. If solutions were oscillatory, maximum plankton concentrations over all depths, over the last 200 days of a simulation were used. C_{max} represents the maximum concentration of each of the plankton components (P_1 , P_2 , Z_1 and Z_2). For the five grazing functions as indicated; (a-e) $P_{1\text{max}}$, (f-j) $P_{2\text{max}}$, (k-o) $Z_{1\text{max}}$ and (p-t) $Z_{2\text{max}}$. The region of q - h parameter space for which all model components had non-negligible concentrations simultaneously is also indicated (u-y). Note that N_1 and N_2 had non-negligible concentrations throughout q - h parameter space with every simulation.

model solutions was largely dependent on the choice of grazing function. For all grazing functions, when predation on mesozooplankton was high, the mesozooplankton component had negligible concentrations, and microzooplankton became the dominant grazer in the system. When implementing grazing functions I, II and IV, the maximum concentrations of each plankton component were similar throughout q and h parameter space. In each instance, there was a clear boundary between two predominant forms. When predation on mesozooplankton was medium to high, solutions predominantly comprised large phytoplankton, microzooplankton, nitrate and ammonium. When the predation on mesozooplankton was low, solutions were dominated by small phytoplankton, mesozooplankton, nitrate and ammonium. It was rare for both phytoplankton size classes to simultaneously have non-negligible concentrations. As such, there was only a narrow region, corresponding to intermediate predation, where all six model

components could simultaneously coexist. With function III, both large and small phytoplankton thrived simultaneously throughout the parameter space examined, and microzooplankton concentrations were negligible only in a small region of parameter space when predation on mesozooplankton was very low. When grazing function V was implemented, model solutions comprised both small and large phytoplankton and microzooplankton in non-negligible concentrations for all parameter space examined.

Irrespective of which of the grazing functions were implemented, steady state solutions could not be found for some regions of the q - h parameter space examined (Fig. 6a-e). Model trajectories that did not reach a steady equilibrium solution described closed limit cycles, wherein the population numbers underwent well-defined cyclic changes in time. No examples of chaotic model solutions were found throughout the parameter space

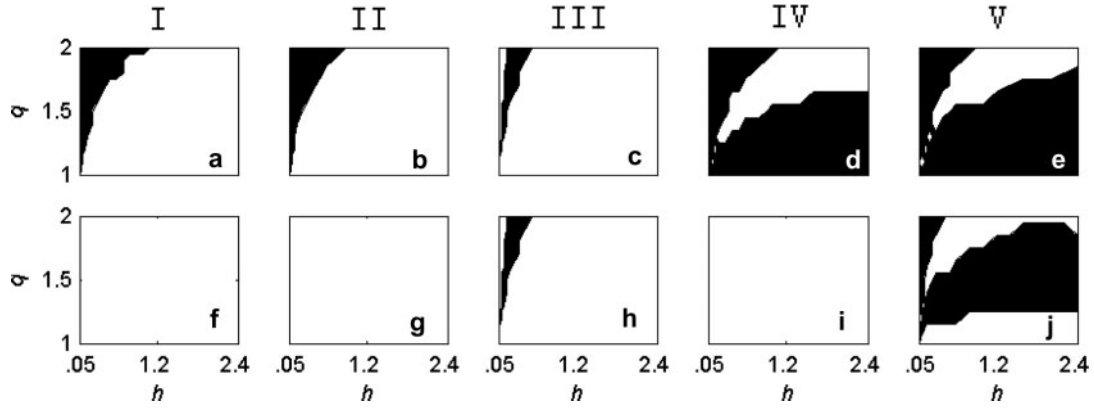


Fig. 6. The classification of model solutions over q ($1 \leq q \leq 2$) and h [$0-2.4$ (g C m^{-3}) $^{1-q} \text{ day}^{-1} = 0.04^{(q-1)} - 0.1908^{(q-1)}$ (mmoles N m^{-3}) $^{1-q} \text{ day}^{-1}$] parameter space. Regions of q - h space where model solutions were at steady equilibrium (shaded black) and were at limit cycles (white) for each of the five grazing functions: (a) function I, (b) function II, (c) function III, (d) function IV and (e) function V. Regions of q - h space where model solutions reached a steady equilibrium and where all six model components were simultaneously non-negligible are also shown (shaded black): (f) function I, (g) function II, (h) function III, (i) function IV and (j) function V.

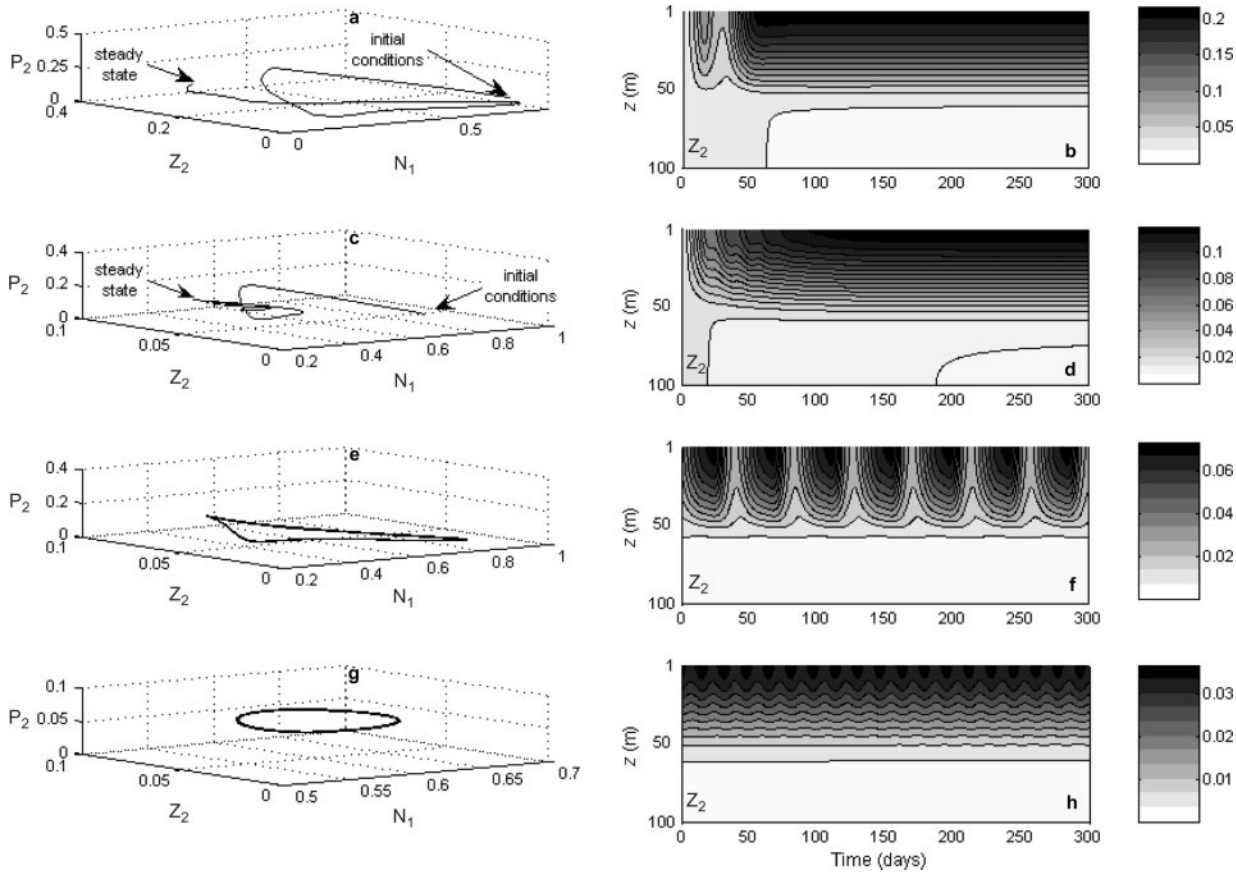


Fig. 7. Examples of steady and non-steady solutions illustrated by three-dimensional (N_1 , P_2 and Z_2) phase space diagrams and corresponding time series solution for Z_2 . (a and b) Steady solution when grazing function = III, $q = 2$ and $h = .4$, (c and d) steady solution when grazing function = V, $q = 2$ and $h = .4$, (e and f) limit cycle solution when grazing function = III, $q = 2$ and $h = 1.4$ and (g and h) limit cycle solution when grazing function = V, $q = 2$ and $h = 1.4$. Note that in the case of limit cycle solutions, the transient behaviour is not shown.

examined for any of the grazing functions implemented. With each grazing function, as q and h were varied, there was at least one clear Hopf bifurcation, where the qua-

litative form of the solution shifted between attraction to a steady equilibrium (e.g. Fig. 7a-d) and a periodic limit cycle (e.g. Fig. 7e-h). With grazing functions I, II and

III, steady solutions could not be found for the majority of the parameter space (Fig. 6a–c). With each of these model variants, when the total predation on mesozooplankton (H) was medium to high, model trajectories were oscillatory. As predation became relatively small, there was a Hopf bifurcation with a transition to steady solutions. In the case of grazing function III, at very low predation, a second bifurcation returned solutions to an oscillatory regime (Fig. 6c). With grazing functions IV and V, model solutions reached a steady state for much of the parameter space examined (Fig. 6d and e). In both cases, there were, however, still two clear Hopf bifurcations as q and h were varied. With these two model variants, we found model solutions to be steady at high predation, to undergo a bifurcation to oscillatory behaviour in the region of intermediate predation and to undergo a second bifurcation back to a steady regime at low predation.

The non-linear dynamics of model solutions correlated well with their structural composition. With grazing functions I and II, solutions that comprised only small phytoplankton, mesozooplankton, nitrate and ammonia were generally steady, while solutions that predominantly comprised large phytoplankton, microzooplankton, nitrate and ammonia were oscillatory. The narrow regions of parameter space that did comprise all model components in non-negligible concentrations (Fig. 5u and v) were non-steady (Fig. 6f and g). Models with grazing function IV had steady equilibrium solutions at both high and low H . In the region of low H (upper left portion of q – h space), solutions were dominated by small phytoplankton, mesozooplankton, nitrate and ammonia (Fig. 5). In the region of high H (lower right portion of q – h space), large phytoplankton, microzooplankton, nitrate and ammonium dominated the solutions. Solutions that comprised all six state variables in non-negligible concentrations were, again, rare (Fig. 5x) and oscillatory (Fig. 6d). Steady equilibrium solutions comprising all six model components in non-negligible concentrations were found only when implementing functions III and V (Fig. 6h and j). The region of steady, permanent coexistence was much broader with grazing function V than with grazing function III.

The time series of the model components in oscillatory solutions showed similarities for each of the grazing functions implemented. With grazing functions I and II, oscillatory solutions generally comprised nitrate, ammonium, large phytoplankton and microzooplankton. An increase in large phytoplankton concentration was followed respectively by a draw down of the nitrate, a slight increase in ammonium concentration, an increase in the microzooplankton concentration and a more rapid increase in the ammonium concentration. The rising grazing pressure from the

microzooplankton caused a crash in the large phytoplankton population, followed by a crash in microzooplankton and ammonium concentrations, respectively. Nitrate, which had started to rise following the increase in ammonium, reached its maximum when the phytoplankton concentration was at a minimum. When all six model components persisted, the small and large phytoplankton oscillated in phase, although a short lag between the increase in small phytoplankton and the increase in large phytoplankton was observed with function II. When mesozooplankton were present, the rise and fall in their concentration lagged that of the microzooplankton. With function IV, when both phytoplankton groups persisted, the extent of predation on mesozooplankton determined which size class ‘bloomed’ first. At lower predation, small phytoplankton would respond before the large phytoplankton, while at high total predation, the opposite was true. With grazing functions III and V, oscillatory solutions comprised all six model components and exhibited a similar temporal progression to that described above.

In reality, because of their different responses to the physical environment, i.e. the light and nutrient field, the phytoplankton size groups will exhibit different seasonal trends in expansion and decline. However, in most, if not all, marine environments, multiple size classes of phytoplankton and zooplankton are often found to coexist simultaneously, for at least a portion of the seasonal cycle. In general, although individual species do disappear over a seasonal cycle, we do not expect the aggregate to disappear. In some regions of the world’s ocean, however, because of the influence of the prevailing physical dynamics, it becomes acceptable to characterize the ecosystem as comprising one dominant phytoplankton size class and one dominant zooplankton size class. For example upwelling systems are generally dominated by large phytoplankton and mesozooplankton. A successful marine ecosystem model should be capable of simulating an ecosystem in which multiple size classes can prevail, and it should be the prescribed forcing to which the ecosystem model is subjected that determines the composition of the model solution. Simulating temporal coexistence of multiple phytoplankton or zooplankton groups can be notoriously difficult. Although equilibrium coexistence of model components, as determined here, is not necessarily the same as the temporal coexistence, our results provide a good indication of which grazing functions are likely to be successful at simulating temporal coexistence for at least part of the seasonal cycle. As we were only able to find solutions which comprised all model components for a narrow region of parameter space when implementing grazing functions I, II and IV, we did not consider these model variants further in this investigation. We focus on comparing and contrasting solutions obtained when implementing grazing functions

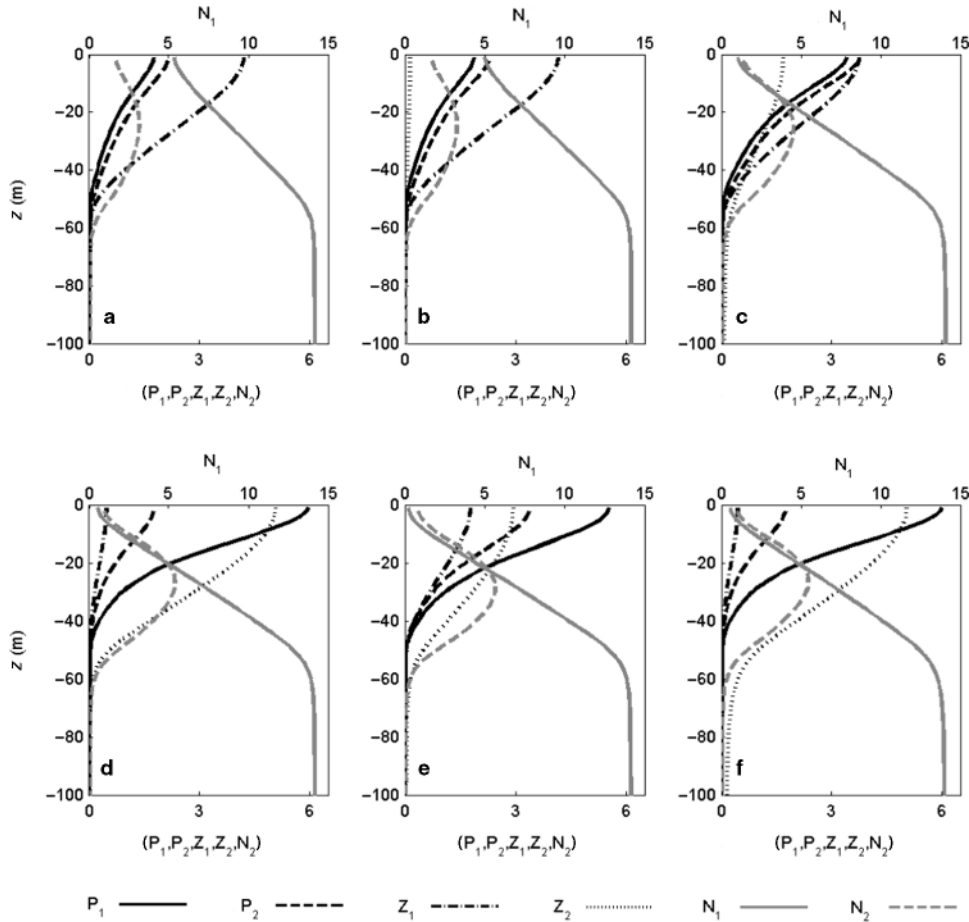


Fig. 8. Equilibrium depth profiles of scaled concentration, when implementing grazing function V with (a) $h = .06$ and $q = 1$, (b) $h = .06$ and $q = 1.5$, (c) $h = .06$ and $q = 2$ and when implementing grazing function III with (d) $h = .06$ and $q = 1.5$, (e) $h = .1$ and $q = 1.5$ and (f) $h = .1$ and $q = 2$. Note that the nitrate (N_1) profile is plotted on a different scale for clarity.

III and V because these model variants are capable of producing solutions comprising all model components for the majority of parameter space examined.

All steady equilibrium solutions obtained when implementing grazing functions III and V had vertical profiles that shared many features (e.g. Fig. 8). In each instance, nitrate concentration was low in the surface mixed layer but increased with depth to dominate the system below the bottom of the mixed layer. Conversely, the concentration of all plankton components decreased with depth from maximum values at the surface. Ammonium always exhibited a sub-surface maximum close to the midpoint of the euphotic zone ($2.3/k_{\text{exd}}$). Although small and large phytoplankton and microzooplankton did not persist much below the bottom of the mixed layer (40 m), mesozooplankton, when present at steady state, persisted far below this.

Despite these general commonalities, the vertical profiles as q and h space were traversed, differed quite

markedly with the two grazing functions. Rather than presenting the full vertical profile for each steady solution, the change in concentration of each model component with q and h at 10 m depth is used to illustrate changes to the complete vertical profile with these parameters. Changes to the concentration of model components at this depth were representative of the trends exhibited at all depths. With both grazing functions III and V, when mesozooplankton concentrations were negligible (q close to 1), variations in h had little influence on model solutions. With grazing function III, there was only a small region of parameter space where the model produced steady equilibrium solutions (Fig. 9). There was nowhere within this region that the vertical profiles could be considered to remain constant with h . With this grazing function, there were no steady solutions when predation was linear ($q = 1$), but as q was increased and the Hopf bifurcation traversed, the vertical concentration profiles for each steady solution varied smoothly but markedly as h varied. Within this

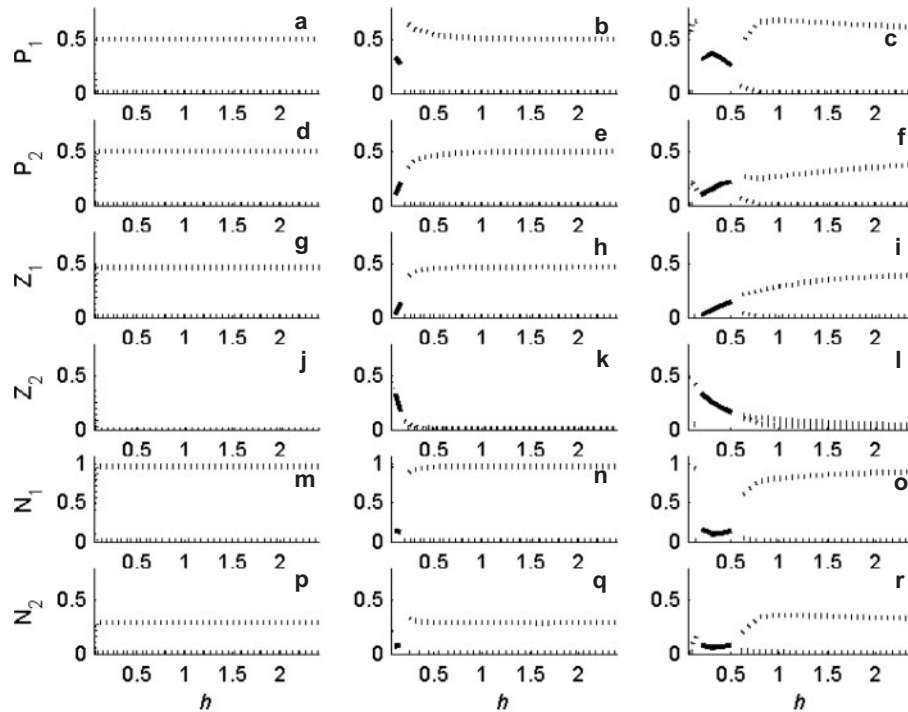


Fig. 9. Bifurcation diagrams when grazing function III is implemented. For $q = 1, 1.5$ and 2 as indicated. (a-c) P_1 , (d-f) P_2 , (g-i) Z_1 , (j-l) Z_2 , (m-o) N_1 and (p-r) N_2 . The dotted lines indicate the maximum and minimum concentrations reached during the cycle of an oscillatory solution. The solid line indicates the equilibrium concentration reached in steady solutions. Data shown are for the 10-m depth level.

steady region, increasing h resulted in an increase followed by a decrease in P_1 , an overall increase in P_2 and Z_1 , a decrease in Z_2 , and a slight decrease followed by a slight increase in N_1 and N_2 . With grazing function V, there were two regions of parameter space, on either side of the Hopf bifurcation, where the model had steady solutions. Within the first region (high total predation), concentrations of each model component varied very little with q or h , even approaching the first Hopf bifurcation (Fig. 10). As mentioned previously, this is in large part due to the low concentrations of mesozooplankton in this region. Throughout this region, the vertical profile closely resembled those shown in Fig. 8a and b. Both phytoplankton size fractions had similar vertical profiles, although the concentration of P_2 exceeded that of P_1 at every depth. Concentrations of Z_1 were approximately twice that of the phytoplankton at every depth. Z_2 had negligible concentrations throughout the water column. Following the second Hopf bifurcation, moving into the region of low predation, model components reached alternative steady states. Within this second region of steady solutions, the vertical profiles of each model component changed smoothly but rapidly with q and h . Moving away from the bifurcation (increasing q , decreasing h), there was an

overall decrease in P_2 , Z_1 , N_1 and N_2 , and an overall increase in P_1 and Z_2 at each depth within the mixed layer.

The non-steady solutions obtained with both grazing functions III and V also provide an insight into the fundamental dynamics of the two model variants. With function V, the maximum and minimum concentrations of each model component reached during a limit cycle varied smoothly and continuously with h and q as the Hopf bifurcation was traversed (Fig. 10). With function III, in the region of medium to low predation, away from the Hopf bifurcation, the maximum concentrations of each of the model components reached during the limit cycles remained relatively constant as h was increased (Fig. 9). The amplitude of limit cycles obtained with function III tended to be much greater than those obtained with function V. In the former case (function III), the concentrations of model components tended to oscillate between a maximum (approaching 1 in the case of nitrate) and negligible concentrations. In the latter case (function V), the maximum concentration attained by any of the model components was smaller than the equivalent model with grazing function III, and the minimum values were always non-negligible. This difference in oscillation amplitude can also clearly be seen in the phase space plots of limit cycle solutions (Fig. 7c and d).

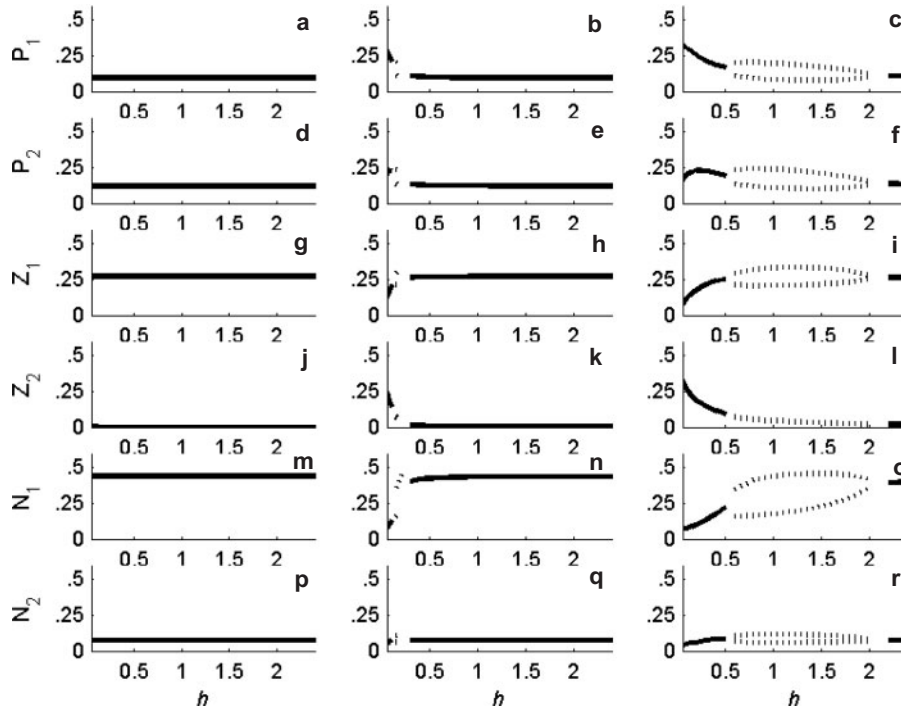


Fig. 10. As for Fig. 9 but with grazing function V implemented.

Sensitivity to parameter values and initial conditions

Past studies have shown that model dynamics can be sensitive to both parameterization and initial conditions (Popova *et al.*, 1997; Edwards and Yool, 2000). In the Gulf of Alaska, the maximum photosynthetic growth, P_{\max} , was found to be equivalent for both phytoplankton size fractions (Strom *et al.*, 2001). With an alternate size division, or in other ecosystems, this may not be so (Furnas, 1990). To see how the model dynamics presented above would be impacted by a change in this parameter, we held the initial conditions and all other parameter values constant, but decreased the maximum photosynthetic growth for large phytoplankton ($P_{\max 2}$) to 1 day^{-1} , half that for the small phytoplankton. We explored the model dynamics over a coarse resolution q - h parameter space for the structurally most dissimilar grazing functions, I and V. Patterns of dynamical model behaviour were found to be similar to those presented above. Model solutions generally came to oscillatory limit cycle solutions with grazing function I and steady equilibrium solutions with function V. The locations of the Hopf bifurcations, in both instances, were similar to those found with the original model parameterization. With grazing function V, the structural composition of model solutions was also similar to that arising with the original parameterization. With grazing function I and the alternative parameterization of P_{\max} model solutions

comprised small phytoplankton throughout q - h space, while large phytoplankton had negligible concentrations.

To test the sensitivity of our model to initial conditions, we doubled the initial nitrate concentration from 10 to 20 mmoles m^{-3} . All other initial concentrations and parameter values were as for the original model. Again, with grazing functions I and V, the patterns of model behaviour were little changed to those presented for the original model. The notable difference was the presence of a second Hopf bifurcation at low total predation (H) when implementing grazing function I. With both grazing functions I and V, the structural composition of model solutions, with respect to survivorship of model components, was little different to that presented for the original initial conditions.

DISCUSSION

This investigation explored the non-linear dynamics of a depth explicit, one-dimensional, six-component marine ecosystem model in which zooplankton could graze on multiple nutritional resources. The model was parameterized for the coastal Gulf of Alaska ecosystem, and was subjected to stationary physical forcing. We systematically varied the specific predation rate [$h = 0.05$ – $2.4 \text{ (g C m}^{-3})^{1-q} \text{ day}^{-1} = 0.04^{(q-1)} - 0.1908^{(q-1)} \text{ (mmoles N m}^{-3})^{1-q} \text{ day}^{-1}$], the form of the predation function ($1 \leq q \leq 2$) and the form of the grazing function.

Classic stability analysis has been used to investigate the dynamical behaviour of simple NPZ models (Franks *et al.*, 1986; Edwards and Brindley, 1999; Edwards *et al.*, 2000), and more complex models that retain the assumption of a homogeneous mixed layer (Ryabchenko *et al.*, 1997; Armstrong, 1999). Such studies have provided the foundation for understanding NPZ model dynamics. However, it is essential that we extend this knowledge to the more complex marine ecosystem models now commonly used in ecosystem studies. It is not possible to find an analytical solution to our intermediately complex, spatially explicit model. Therefore, the classic approach to stability analysis, determination of the eigenvalues of the Jacobian (community) matrix, was of limited use for classifying model behaviour. Despite this obstacle, it is important to gain an appreciation of the dynamics of such complex systems. Therefore, we examined model trajectories in time and space, numerically seeking and classifying model solutions. This analysis provides a useful insight into behaviour of models where zooplankton grazers, subjected to a depth explicit mixing profile, can feed on a mixed prey field.

The total predation ($H = h \cdot Z_2^q$) experienced by the mesozooplankton and the form of the grazing function played an important role in governing the non-linear dynamics of this intermediately complex ecosystem model. In agreement with past investigations using simpler NPZ models (Edwards and Bees, 2001), we found that limit cycles can be found for all predation exponents and are not exclusively a result of using a linear ($q = 1$) form of predation. With each of the five grazing functions, we found Hopf bifurcations spanning the q and h parameter space, where the form of the solution transitioned between steady equilibrium and periodic limit cycles. A three-component, one-predator, one-prey model with a sigmoidal grazing function has been shown to have two Hopf bifurcations that span q and h space bounding a region of limit cycle behaviour (Edwards and Bees, 2001). We have shown that sigmoidal grazing functions extended to multiple nutritional resources (functions IV and V) give rise to similar patterns of bifurcations in our more complex model (Fig. 6d and e). Additionally, we have shown that Hopf bifurcations also exist when implementing alternative extensions of the Michaelis–Menten grazing function to multiple nutritional resources (functions I, II and III). With these functional forms, however, limit cycle behaviour was found to be the more prevalent form for model solutions. Only in a narrow region of parameter space did these grazing functions give rise to steady equilibrium solutions. This pattern of behaviour, with a region of stable steady states surrounded by two regions of oscillations, is interesting because it is opposite to that found previously (Edwards and Bees, 2001). It is interesting to note that while we

found Fasham's switching grazing model (grazing function III) to only rarely produce models that were dynamically stable, Armstrong (Armstrong, 1999) found that a model with 'distributed grazing' being modelled at a community level for a single zooplankton species was dynamically stable under a wide range of conditions. There have been only a few observations of oscillatory population dynamics in nature, e.g. those by Williams (Williams, 1988) at Ocean Weather Station India. If such oscillations do exist, the general lack of supporting observations could be a result of a sampling resolution that is insufficient to capture short-term transient dynamics, or could be because of a dampening effect that species succession or physical advection has on the overall population dynamics. Whether or not such oscillations are thought to exist in reality, our findings, which illustrate the likelihood of and oscillatory/steady solution arising from the predator prey interactions defined by the alternative grazing functions, will be a useful resource during model development and analysis.

Because of their different responses to the physical environment, i.e. the light and nutrient field, the phytoplankton size groups will, in reality, exhibit different seasonal trends. Observational data, however, commonly show coexistence of multiple phytoplankton and zooplankton size classes, at least for part of the seasonal cycle. Simulating coexistence of model components, although notoriously difficult, is, therefore, an important constraint for ecosystem models that comprise multiple grazers and multiple prey types. Permanent coexistence of model components at equilibrium was strongly influenced by the choice of grazing function. It was rare for all predators and prey to exist simultaneously when implementing I, II and IV. This is in line with the conclusions by Armstrong (Armstrong, 1994), that such concave down functions tend to promote prey elimination. Although functions II and IV do have regions that will decrease or prevent entirely the elimination of rare prey, these reprises from zooplankton grazing do not come into effect until the total prey concentration has fallen below a critical level. With all three of these grazing functions, under the stationary forcing regime implemented, the system typically purges itself until only one predator and one prey remain. Generally, if predation on mesozooplankton followed a function that was quadratic, or close to it, the mesozooplankton were able to thrive, and microzooplankton and large phytoplankton were eliminated through competitive exclusion (mesozooplankton had higher affinity for these prey items). However, if predation on mesozooplankton approached a linear functional form, mesozooplankton approached negligible concentrations, and the microzooplankton became the dominant grazer and small phytoplankton

were eliminated through competitive exclusion (microzooplankton had a higher affinity for this phytoplankton size class). The non-linear dynamics of the remaining four-component system was determined by the efficiency of the remaining grazer to capture the remaining prey. If the grazer was able to eat a large proportion of the prey (i.e. microzooplankton grazing on large phytoplankton), the resulting solution tended to be periodic. Conversely, if the grazer could eat only a small proportion of the prey (i.e. mesozooplankton grazing on small phytoplankton), a steady equilibrium was generally reached. With all three of these grazing functions, all six model components were able to coexist only in a narrow region defined by an intermediate level of total predation (H) on the mesozooplankton. Grazing functions III and V allow 'prey switching', with zooplankton eating a disproportional amount of the abundant prey. When multiple nutritional resources are present, both of these functional response curves have regions where rare prey experiences a reprise from grazing, even if the concentration of other available prey sources is relatively high. This ability of the zooplankton grazers to 'switch' prey enhances the likelihood that all plankton components will survive simultaneously (Hutson, 1984; Strom and Loukos, 1998) and so decreases the likelihood of prey elimination through competitive exclusion. Equilibrium coexistence of model components resulting from a stationary forcing regime is not necessarily the same as temporal coexistence and so could be misleading as to the true effectiveness of a model to correctly simulate the observed seasonal cycle. Nevertheless, the results presented here do still provide a good indication of which grazing functions are likely to be successful at simulating temporal coexistence for at least part of the seasonal cycle, i.e. functions III and V which provide rare prey with a refuge from grazing regardless of the concentration of other available prey types. It is important to note, however, that given a seasonal forcing regime, more success may be achieved with grazing functions I, II and IV.

This investigation focused on grazing functions III and IV because they produced solutions that comprised all model components and were steady, for at least some of the q - h parameter space examined. Balancing the best form of a grazing function from a modeller's point of view and from an observationalist's point of view can present a challenge. An observationalist may seek a form that appears to best describe the grazer under investigation. However, usually only one, or a few, species are considered at a time. Conversely, because of the necessary aggregation that modellers perform when seeking to describe an ecosystem, such a functional form may not be appropriate. Often, trophic levels rather than individual

species are considered, and so certain functional forms may not make sense from a biological point of view. Additionally, the elimination of model components or the production of oscillatory model solutions are generally considered undesirable traits, and a grazing function that promotes such behaviour would be less favoured, although we stress that this may be due purely to modelling convenience. It could be potentially argued that, oscillatory solutions are just as realistic as steady solutions. Short-term oscillations in plankton have been observed for a few marine and freshwater ecosystems (Ryabchenko *et al.*, 1997; Edwards, 2001). However, because of inadequate sampling resolution, we do not have a clear understanding of whether components of the coastal Gulf of Alaska ecosystem exhibit unforced oscillations in biomass. As with most observational studies, observational data in this region are not of a sufficiently high temporal resolution that they would capture short-term oscillations in ecosystem components such as those described above. Model solutions exhibiting unforced oscillations are, however, often considered undesirable because it makes it more difficult to discern any longer term periodicity (seasonal signal, annual, etc.).

There is much discussion in the literature with regard to the realism of different forms of grazing function. For example there are many instances of switching reported (Kioerboe *et al.*, 1996; Gismervik and Andersen, 1997; Martin-Cereceda *et al.*, 2003), however, although microzooplankton have been shown to exhibit selective feeding, they do not necessarily alter their feeding behaviour in response to a changing prey field, so stable prey trajectories are not necessarily observed under experimental conditions (Strom and Loukos, 1998). It is important to carefully consider the inherent assumptions behind a grazing function, particularly with functions that describe grazing on multiple nutritional resources, as they are not always obvious at first glance (Gentleman *et al.*, 2003). In fact the use of some popular grazing functions, which include active selection of abundant prey (Class 3 multiple functional responses), is advised against because they have been found to produce wide regions of anomalous dynamics such as a decrease in total nutritional intake with an increase in resource density (Gentleman *et al.*, 2003). Although function III investigated here falls within this class, with our chosen model parameterization no such anomalous behaviour was observed. Despite the potential for anomalous behaviour, we chose to include this grazing function in our investigation because since its implementation in the classic Fasham model (Fasham *et al.*, 1990) it has become a commonly used function in models with multiple prey types (Chai *et al.*, 1996; Loukos *et al.*, 1997; Pitchford and Brindley, 1999).

Model dynamics are known to be sensitive to both parameterization and initial conditions (Popova *et al.*, 1997; Edwards and Yool, 2000). Here, we investigated the influence of varying the predation parameters in some detail for a specified set of initial conditions. However, it is important to consider that variation in other parameters or a change to the initial conditions may result in dynamics different to those presented here. Our preliminary investigation into the influence of varying the maximum photosynthetic growth rate (P_{\max}) for large phytoplankton revealed that the structure of the model solutions (i.e. the coexistence of model components) was impacted by variation in this parameter but the location of Hopf bifurcations across q - h space went virtually unchanged. Additionally, we have shown that similar patterns of dynamics persisted even when doubling the initial nitrate concentration. From these results, it is difficult to draw any conclusions regarding the model's sensitivity to variations in other parameter values, or to initial conditions very different to those used here. It has been shown, however, that a three-component, one-predator, one-prey model with sigmoidal grazing has Hopf curves that remain fairly similar as many of the other model parameters are varied (Edwards and Brindley, 1999). This suggests, but remains for further study, that varying additional model parameters within our six-component model would result in a similar pattern of dynamical behaviour.

In an effort to keep our model as simple as possible while allowing zooplankton to graze on multiple nutritional resources, we used the simplest form of many of the biological process functions that were not directly under investigation here. This included a gross simplification of the nutrient regeneration loop through the exclusion of an explicitly modelled detritus component. The assumption of instantaneous remineralization of organic material ensured a continual supply of nutrient utilizable by the phytoplankton. Despite our simplification of the nutrient regeneration loop, our model is far more likely to exhibit limit cycle behaviour with some grazing functions than with others. Many biological models currently used in ecosystem studies incorporate a more explicit representation of the regeneration loop, although the degree of detail incorporated varies widely. The more complex models include both particulate organic matter (POM) and dissolved organic matter (DOM) as separate state variables (Kishi, 2000), and some even specifically represent bacteria (Lancelot *et al.*, 2000). Other models have a single 'detrital' component which is assumed to comprise both POM and DOM (Loukos *et al.*, 1997; Denman and Peña, 2002). The inclusion of a detritus component delays the return of organic matter to inorganic nutrients, decreasing the

total nutrient available at any instant in the system. Such a nutrient store could also be exported from the mixed layer, via sinking, prior to remineralization. By reducing the amount of readily available nutrient, the addition of detritus to the model could potentially act as a 'brake' on the system by acting as a delay term. The influence of such a delay term is, at present, unclear. It has been shown that a high nutrient supply (caused by high entrainment into the mixed layer of high pycnocline nutrient concentrations) can enhance the susceptibility to oscillatory behaviour (Popova *et al.*, 1997). This would suggest that the addition of a detritus component would act to dampen model oscillations. Edwards (Edwards, 2001) has, however, shown that the addition of detritus to a three-component NPZ model had little consequence for model dynamics, provided zooplankton were unable to graze on the detritus. An inability of zooplankton to graze on detritus is often assumed in ecosystem models (Leonard *et al.*, 1999; Chifflet *et al.*, 2001; Kishi *et al.*, 2001), however, while detritus may not form a large portion of the zooplankton diet, at least some species of zooplankton do graze on detritus (Paffenhöfer and Knowles, 1979; Poulet, 1983). This assumption, therefore, may need further consideration. It is clear that the influence of a more explicit representation of the nutrient regeneration loop on model dynamics requires further investigation. It is possible that the addition of a sinking detritus component to a depth explicit model could have a notable influence on model dynamics. Self-shading by the phytoplankton was another biological process that was not included in our model but could potentially influence model dynamics. We did find, however, that both functions IV and V, multi-resource versions of the sigmoidal grazing function, produced a pattern of steady per limit cycle behaviour across q - h parameter space which was very similar to that found for a three-component NPZ model that did include self-shading for the phytoplankton (Edwards and Bees, 2001). This suggests that the dynamics presented here result primarily from the predator-prey interactions dictated by the alternate grazing functions, rather than from enhanced excitability owing to our omission of self-shading.

The existence of chaos in marine ecosystem models has been well documented (Popova *et al.*, 1997; Edwards and Bees, 2001). For a one-predator, two-prey ecosystem, with a grazing function equivalent to function V, model solutions have been shown to exhibit chaotic behaviour when forced externally with an annual physical cycle (Popova *et al.*, 1997). With the stationary physical forcing (light level and mixing curve) used in this investigation, we did not find any examples of chaotic solutions for any of the grazing functions tested. A finer

resolution exploration of q - h parameter space may reveal the existence of chaotic solutions for small windows of parameter space. Additionally, variations in physical forcing are known to have a large impact on model dynamics (Ryabchenko *et al.*, 1997; Edwards *et al.*, 2000), and it is possible that the dynamical behaviour observed with stationary forcing could be damped out or enhanced with a seasonally varying forcing regime or with a model with more than one spatial dimension. It has been shown that strong upwelling or a shallow pycnocline, which results in a high nutrient supply, can play an important role in oscillatory behaviour (Popova *et al.*, 1997) and could potentially enhance the excitability of the model (and thus produce more limit cycles or even chaotic behaviour). Within our model, nitrate is mixed into the upper mixed layer only through the action of diffusion. Hence, we have shown that even in the absence of strong upwelling, oscillatory dynamical behaviour can be very prevalent with some grazing functions.

Biological dynamics in the ocean are highly transient, and capturing such transient biological behaviour with an ecosystem model that has a stationary physical forcing is inherently difficult. However, the focus of this study was to try to understand the dynamics of alternative forms of an ecosystem model, parameterized with realistic values, in order to guide future modelling efforts, rather than to replicate observational data. Our findings contribute towards the more general understanding of non-linear dynamics and structural stability of complex marine ecosystem models in which multiple grazers can select from multiple prey types. We have provided an insight into the impact that the choice of commonly used multiple resource grazing functions and mortality functions can have on model dynamics. We are reluctant to suggest that any grazing or mortality function should be chosen over alternatives at this stage, this choice will clearly depend on the assumptions that one is willing to make and on the ecosystem one is trying to simulate. However, if a modeller is selecting for or against a type of behaviour (steady/oscillatory), our findings could provide a useful resource. E.g. if the desire is to achieve a structurally stable model comprising all model components that does not exhibit unforced periodic oscillations, then using grazing function V to simulate zooplankton grazing appears most appropriate. Models in which this grazing function was implemented were also the most robust, i.e. the form of the equilibrium solutions did not change significantly over a realistic range of parameter values, although even this model structure has the ability to produce non-steady solutions for some forms of the predation function. With this grazing function models were more likely to be steady as the predation function tended towards the

linear form, although mesozooplankton were often eliminated in this region of parameter space. With both of these biological process functions, as with any others used in the development of a marine ecosystem model, the modeller will have to ascertain if the assumptions inherent in the formulation are appropriate for the plankton community of interest. Our findings have important implications for modelling efforts in environments where multiple prey and predator classes persist simultaneously. It is hoped that this analysis will be of value during model construction of such ecosystems, and for interpreting results from biophysical model simulations in which the physical forcing is varied over a seasonal cycle.

ACKNOWLEDGEMENTS

We thank three anonymous reviewers for their comments and suggestions, which greatly enhanced our manuscript. G.G.'s contribution to this research was funded through a fellowship from the Rasmuson Fisheries Research Center at the School of Fisheries and Ocean Science, University of Alaska, Fairbanks. The work was performed by G.G. in partial fulfilment of the requirements for a PhD degree at the University of Alaska, Fairbanks. D.M.'s contribution to this work constitutes contribution No. 243 of the U.S. GLOBEC program, jointly funded by the National Science Foundation and National Oceanic and Atmospheric Administration. S.H.'s contribution to this research constitutes contribution FOCI-0537 to NOAA's Fisheries-Oceanography Coordinated Investigations' and GLOBEC Contribution No. 243 of the U.S. GLOBEC/NEP program.

REFERENCES

- Aita, M. N., Yamanaka, Y. and Kishi, M. J. (2003) Effects of ontogenetic vertical migration of zooplankton on annual primary production – using NEMURO embedded in a general circulation model. *Fish. Oceanogr.*, **12**, 284–290.
- Ambler, J. W. (1986) Formulation of an ingestion function for a population of *Paracalanus* feeding on mixtures of phytoplankton. *J. Plankton Res.*, **8**, 957–972.
- Armstrong, R. A. (1994) Grazing limitation and nutrient limitation in marine ecosystems: steady state solutions of an ecosystem model with multiple food chains. *Limnol. Oceanogr.*, **39**, 597–608.
- Armstrong, R. A. (1999) Stable model structures for representing biogeochemical diversity and size spectra in plankton communities. *J. Plankton Res.*, **21**, 445–464.
- Chai, F., Barber, R. T. and S. T. Lindley (1996) Origin and maintenance of high nutrient condition in the equatorial Pacific. *Deep-Sea Res. II*, **42**, 1031–1064.
- Chifflet, M., Andersen, V., Prieur, L. *et al.* (2001) One-dimensional model of short-term dynamics of the pelagic ecosystem in the NW Mediterranean Sea: effects of wind events. *J. Mar. Syst.*, **30**, 89–114.

- Corkett, C. J. and McLaren, I. A. (1978) The biology of *Pseudocalanus*. *Adv. Mar. Biol.*, **15**, 1–231.
- Dagg, M. (1993) Grazing by the copepod community does not control phytoplankton production in the Subarctic Pacific Ocean. *Prog. Oceanogr.*, **32**, 163–183.
- Dagg, M. (1995) Ingestion of phytoplankton by the micro- and mesozooplankton communities in a productive subtropical estuary. *J. Plankton Res.*, **17**, 845–857.
- Dagg, M. J. and Walser, W. E. (1987) Ingestion, gut passage, and egestion by the copepod *Neocalanus plumchrus* in the laboratory and in the subarctic Pacific Ocean. *Limnol. Oceanogr.*, **32**, 178–188.
- Denman, K. L. and Gargett, A. E. (1995) Biological physical interactions in the upper ocean: the role of vertical and small scale transport processes. *Annu. Rev. Fluid Mech.*, **27**, 225–255.
- Denman, K. L. and Peña, M. A. (1999) A coupled 1-D biological/physical model of the northeast subarctic Pacific Ocean with iron limitation. *Deep-Sea Res. II*, **46**, 2877–2908.
- Denman, K. L. and Peña, M. A. (2002) The response of two coupled one-dimensional mixed layer/planktonic ecosystem models to climate change in the NE subarctic Pacific Ocean. *Deep-Sea Res. II*, **49**, 5739–5757.
- Dugdale, R. C. and Goering, J. J. (1967) Uptake of new and regenerated forms of nitrogen in primary productivity. *Limnol. Oceanogr.*, **12**, 196–206.
- Edwards, A. M. (2001) Adding detritus to a Nutrient Phytoplankton Zooplankton model: a dynamical-systems approach. *J. Plankton Res.*, **23**, 389–413.
- Edwards, A. M. and Bees, M. A. (2001) Generic dynamics of a simple plankton population model with a non-integer exponent of closure. *Chaos, Solitons, Fractals*, **12**, 289–300.
- Edwards, A. M. and Brindley, J. (1996) Oscillatory behaviour in a three-component plankton population model. *Dyn. Stabil. Syst.*, **11**, 347–370.
- Edwards, A. M. and Brindley, J. (1999) Zooplankton mortality and the dynamical behaviour of plankton population models. *Bull. Math. Biol.*, **61**, 303–339.
- Edwards, C. A., Powell, T. A. and Batchelder, H. P. (2000) The stability of an NPZ model subject to realistic levels of vertical mixing. *J. Mar. Res.*, **58**, 37–60.
- Edwards, A. M. and Yool, A. (2000) The role of higher predation in plankton population models. *J. Plankton Res.*, **22**, 1085–1112.
- Eppley, R. W. and Peterson, B. J. (1979) Particulate organic matter flux and planktonic new production in the deep ocean. *Nature*, **282**, 677–680.
- Evans, G. T. and Parslow, J. S. (1985) A model of annual plankton cycles. *Biol. Oceanogr.*, **3**, 327–347.
- Fasham, M. J. R. (1995) Variations in the seasonal cycle of biological production in subarctic oceans: a model sensitivity analysis. *Deep-Sea Res. I*, **42**, 1111–1149.
- Fasham, M. J. R., Ducklow, H. W. and McKelvie, S. M. (1990) A nitrogen-based model of plankton dynamics in the oceanic mixed layer. *J. Mar. Res.*, **48**, 591–639.
- Fasham, M. J. R., Sarmiento, J. L., Slater, R. D. *et al.* (1993) Ecosystem behaviour at Bermuda Station 'S' and ocean weather station 'India': a general circulation model and observational analysis. *Global Biogeochem. Cycles*, **7**, 379–415.
- Flynn, K. J. (1999) Nitrate transport and ammonium–nitrate interactions at high nitrate concentration and low temperature. *Mar. Ecol. Prog. Ser.*, **187**, 283–287.
- Flynn, K. J. (2003) Modelling multi-nutrient interactions in phytoplankton; balancing simplicity and realism. *Prog. Oceanogr.*, **56**, 249–279.
- Franks, P. J. S. and Chen, C. (2001) A 3-D prognostic numerical model study of the Georges bank ecosystem. Part II: biological-physical model. *Deep-Sea Res.*, **48**, 457–482.
- Franks, P. J. S., Wroblewski, J. S. and Flierl, G. R. (1986) Behavior of a simple plankton model with food-level acclimation by herbivores. *Mar. Biol.*, **91**, 121–129.
- Frost, B. W. (1972) Effects of size and concentration of food particles on the feeding behavior of the marine planktonic copepod *Calanus pacificus*. *Limnol. Oceanogr.*, **17**, 805–815.
- Frost, B. W. (1975) A threshold feeding behavior in *Calanus pacificus*. *Limnol. Oceanogr.*, **20**, 263–266.
- Frost, B. W. (1987) Grazing control of phytoplankton stock in the open subarctic Pacific Ocean: a model assessing the role of mesozooplankton, particularly the large calanoid copepods *Neocalanus* spp. *Mar. Ecol. Prog. Ser.*, **39**, 49–68.
- Frost, B. W. and Franzen, N. C. (1992) Grazing and iron limitation in the control of phytoplankton stock and nutrient concentration: a chemostat analogue of the Pacific equatorial upwelling zone. *Mar. Ecol. Prog. Ser.*, **83**, 291–303.
- Furnas, M. J. (1990) In situ growth rates of marine phytoplankton: approaches to measurement, community and species growth rates. *J. Plankton Res.*, **12**, 1117–1151.
- Gentleman, W., Leising, A., Frost, B. *et al.* (2003) Functional response for zooplankton feeding on multiple resources: a review of assumptions and biological dynamics. *Deep Sea Res. II*, **50**, 2847–2875.
- Gifford, D. J. and Dagg, M. J. (1988) Feeding of the estuarine copepod *Acartia tonsa* Dana: carnivory vs. herbivory in natural microplankton assemblages. *Bull. Mar. Sci.*, **43**, 458–468.
- Gismervik, I. and Andersen, A. (1997) Prey switching by *Acartia* clause: experimental evidence and implications of intraguild predation assessed by a model. *Mar. Ecol. Prog. Ser.*, **157**, 247–259.
- Hurtt, G. C. and Armstrong, R. A. (1999) A pelagic ecosystem model calibrated with BATS and OWSI data. *Deep-Sea Res. I*, **46**, 27–61.
- Hutson, V. (1984) Predator mediated coexistence with switching predator. *Math. Biosci.*, **68**, 233–246.
- Ivlev, V. S. (1961) *Experimental Ecology of the Feeding of Fishes*. Yale University Press, New Haven.
- Johnson, P. W. and Sieburth, J. M. (1979) Chroococcoid cyanobacteria in the sea: a ubiquitous and diverse photo-trophic biomass. *Limnol. Oceanogr.*, **24**, 928–935.
- Johnson, P. W. and Sieburth, J. M. (1982) In-situ morphology and occurrence of eucaryotic phototrophs of bacterial size in the picoplankton of estuarine and oceanic waters. *J. Phycol.*, **18**, 318–327.
- Jonsson, P. R. and Tiselius, P. (1990) Feeding behaviour, prey detection and capture efficiency of the copepod *Acartia tonsa* feeding on planktonic ciliates. *Mar. Ecol. Prog. Ser.*, **60**, 35–44.
- Kioerboe, T., Saiz, E. and Viitasalo, M. (1996) Prey switching behaviour in the planktonic copepod *Acartia tonsa*. *Mar. Ecol. Prog. Ser.*, **143**, 65–75.
- Kishi, M. J., Motono, H., Kashiwai, M. *et al.* (2001) An ecological-physical coupled model with ontogenetic vertical migration of zooplankton in the northwestern pacific. *J. Oceanogr.*, **57**, 499–507.

- Kleppel, G. S. (1993) On the diets of calanoid copepods. *Mar. Ecol. Prog. Ser.*, **99**, 183–195.
- Kleppel, G. S., Burkart, C. A., Carter, K. *et al.* (1996) Diets of calanoid copepods on the West Florida continental shelf: relationships between food concentration, food composition and feeding activity. *Mar. Biol.*, **127**, 209–217.
- Lancelot, C., Hannon, E., Becquevort, S. *et al.* (2000) Modeling phytoplankton blooms and carbon export production in the Southern Ocean: dominant controls by light and iron in the Atlantic sector in Austral spring 1992. *Deep-Sea Res. I*, **47**, 1621–1662.
- Landry, M. R. and Hassett, R. P. (1982) Estimating the grazing impact of marine micro-zooplankton. *Mar. Biol.*, **67**, 283–288.
- Legendre, L. and Rassoulzadegan, F. (1995) Plankton and nutrient dynamics in marine waters. *Ophelia*, **41**, 153–172.
- Leonard, C. L., McClain, C. R., Murtugudde, R. *et al.* (1999) An iron-based ecosystem model of the central equatorial Pacific. *J. Geophys. Res.*, **104**, 1325–1341.
- Lomas, M. W. and Glibert, P. M. (1999) Temperature regulation of nitrate uptake: a novel hypothesis about nitrate uptake reduction in cool-water diatoms. *Limnol. Oceanogr.*, **44**, 556–572.
- Loukos, H., Frost, B. W., Harrison, D. E. *et al.* (1997) An ecosystem model with iron limitation of primary production in the equatorial Pacific at 140°W. *Deep-Sea Res. II*, **44**, 2221–2249.
- Luick, J. L., Royer, T. C. and Johnson, W. R. (1987) Coastal atmospheric forcing in the northern Gulf of Alaska. *J. Geophys. Res.*, **92**, 3841–3848.
- Malchow, H. (1994) Non equilibrium structures in plankton dynamics. *Ecol. Model.*, **75/76**, 123–134.
- Martin-Cereceda, M., Novarnio, G. and Young, J. R. (2003) Grazing by *Prymnesium parvum* on small planktonic diatoms. *Aquat. Microb. Ecol.*, **33**, 191–199.
- May, R. M. (1972) Limit cycles in predator-prey communities. *Science*, **177**, 900–902.
- May, R. M. (1973) *Stability and Complexity in Model Ecosystems*. Princeton University Press, Princeton, New Jersey.
- Monod, J. (1942) Recherches sur la croissance des cultures bactériennes [studies on the growth of bacterial cultures]. *Actualities Scientifique Industrielles*, **911**, 1–215.
- Mullin, M. M. and Fuglister, F. J. (1975) Ingestion by planktonic grazers as a function of concentration of food. *Limnol. Oceanogr.*, **20**, 259–262.
- Murdoch, W. W. (1973) The functional response of predators. *J. Appl. Ecol.*, **10**, 335–354.
- Oaten, A. and Murdoch, W. W. (1975) Switching, functional response, and stability in predator-prey systems. *Am. Nat.*, **109**, 299–318.
- Paffenhöfer, G. A. and Knowles, S. C. (1979) Ecological implications of fecal pellet size, production and composition by copepods. *J. Mar. Res.*, **37**, 35–49.
- Pitchford, J. W. and Brindley, J. (1999) Iron limitation, grazing pressure and oceanic high nutrient-low chlorophyll (HNLC) regions. *J. Plankton Res.*, **21**, 525–547.
- Popova, E. E., Fasham, M. J. R., Osipov, A. V. *et al.* (1997) Chaotic behaviour of an ocean ecosystem model under seasonal external forcing. *J. Plankton Res.*, **19**, 1495–1515.
- Poulet, S. A. (1983) Factors controlling utilization of nonalgal diets by particle-grazing copepods: a review. *Oceanol. Acta*, **6**, 221–234.
- Redfield, A. C., Ketchum, B. K. and Richards, F. A. (1963) The influence of organisms on the composition of sea-water. *Sea*, **2**, 26–77.
- Riley, G. A. (1946) Factors controlling phytoplankton populations on Georges Bank. *J. Mar. Res.*, **6**, 54–72.
- Ryabchenko, V. A., Fasham, M. J. R., Kagan, B. A. *et al.* (1997) What causes short-term oscillations in ecosystem models of the ocean mixed layer? *J. Mar. Res.*, **13**, 33–50.
- Steele, J. H. (1974) *The Structure of Marine Ecosystems*. Harvard University Press, Cambridge.
- Steele, J. H. and Henderson, E. W. (1992) The role of predation in plankton models. *J. Plankton Res.*, **14**, 157–172.
- Strom, S. L. (1991) Growth and grazing rates of the herbivorous dinoflagellate *Gymnodinium* sp. from the open subarctic Pacific Ocean. *Mar. Ecol. Prog. Ser.*, **78**, 103–113.
- Strom, S. L., Brainard, M. A., Holmes, J. L. *et al.* (2001) Phytoplankton blooms are strongly impacted by microzooplankton grazing in coastal North Pacific waters. *Mar. Biol.*, **138**, 355–368.
- Strom, S. and Loukos, H. (1998) Selective feeding by protozoa: model and experimental behaviors and their consequences for population stability. *J. Plankton Res.*, **20**, 831–846.
- Strom, S. L. and Welschmeyer, N. A. (1991) Pigment-specific rates of phytoplankton growth and microzooplankton grazing in the open subarctic Pacific Ocean. *Limnol. Oceanogr.*, **36**, 50–63.
- Weingartner, T., Coyle, K., Finney, B. *et al.* (2002) The Northeast Pacific GLOBEC Program: Coastal Gulf of Alaska. *Oceanography*, **15**, 48–63.
- Williams, R. (1988) Spatial heterogeneity and niche differentiation in oceanic zooplankton. In Boxshall, G. A. and Schimke, H. K. (eds), *Biology of Copepods. Hydrobiologia*, **167/168**, 151–159.
- Wroblewski, J. S. (1977) A model of phytoplankton plume formation during variable Oregon upwelling. *J. Mar. Res.*, **35**, 357–394.
- Yool, A. (1998) The dynamics of open-ocean plankton ecosystem models. PhD Thesis. University of Warwick.

